
# ISSC 2018 Committee V.3 - Materials and Fabrication Technology

*Proceedings of the 20th International Ship and Offshore Structures Congress (ISSC 2018) Volume II – M.L. Kaminski and P. Rigo (Eds.)*

*doi:10.3233/978-1-61499-864-8-143*

**COMMITTEE V.3**

# MATERIALS AND FABRICATION TECHNOLOGY

## COMMITTEE MANDATE

The committee shall give an overview about new developments in the field of ship and offshore materials and fabrication techniques with a focus on trends which are highly relevant for practical applications in the industry in the recent and coming years. Particular emphasis shall be given to the impact of welding and corrosion protection techniques for structural performance, and on the development of lighter structures.

## AUTHORS/COMMITTEE MEMBERS

Chairman: Lennart Josefson, *Sweden*
Stephen van Duin, *Australia*
Bianca de Carvalho Pinheiro, *Brazil*
Nana Yang, *China*
Luo Yu, *China*
Albert Zamarin, *Croatia*
Heikki Remes, *Finland*
Frank Roland, *Germany*
Marco Gaiotti, *Italy*
Naoki Osawa, *Japan*
Agnes Marie Horn, *Norway*
Myung Hyun Kim, *South Korea*
Brajendra Mishra, *USA*

## KEYWORDS

Lightweight, composites, adhesive, welding, residual stress, distortions, fatigue, steels, arctic, qualification, approval, high frequency mechanical impact (HFMI)

**CONTENTS**

## 1. INTRODUCTION

This report presents recent developments in materials and fabrication technology in the shipping and offshore fields. This field is under strong pressure due to a decline in orders in particular in the offshore sectors, and also a drop in new build prices. But this also drives a strong development of new materials, fabrications processes and also means for qualifying and approving new materials and processes.

Chapter 2 shows recent trends in ship and offshore production, and in research in these fields, primarily publicly funded. The development of new metallic materials and composites are dealt with in Chapter 3. Chapter 4 gives an overview of welding methods for steels, and fabrication of composites, as well as advances in additive manufacturing. One new area for this Committee is the work with qualification and approval of new materials and processes. This is discussed in Chapter 5 with special focus on approval of composites, what tests are needed for approval and how can this be carried out in an efficient and time-consuming manner.

The V.3 Committee reports three benchmarks, the first is a continuation of the benchmark in the ISSC 2015 V.3 report, welding of a stiffener to a plate (T-Joint) and reports FE-computed residual stresses and deformations, which are compared with experimental results. It gives guidelines for the use of both heat source and model parameters. The second benchmark deals with a single carbon / steel lap joint using a specific adhesive. The sensitivity of parameters that define the separation law for the adhesive on the debonding of the single lap joint is assessed. Computed results are compared with experimental results, and some aspects of material modelling is discussed. The third benchmark deals with fatigue life improvement of fillet welds by use of HFMI (High Frequency Mechanical Impact) treatments. Based on a test case, peening of a stress-free flat steel plate, a best practice guide for simulating a HFMI treatment is given including the use of material model and element mesh size.

The Committee's mandate includes corrosion protection techniques. However, as this topic was covered extensively in the previous 2015 Committee report, it was decided not cover this area in the current report.

## 2. GENERAL TRENDS

The shipping market has seen a continued decrease in new orders in 2015 and 2016. This fall in orders is combined with a strong drop in new building prices. Figure 1 (total) and Table 1 (broken down in ship categories) clearly show this change in new orders. It is seen that the low order intake during the last years is not equally distributed over all maritime markets. While the orders for standard transport ships (tanker, bulk, container) has partly dramatically decreased, orders for RoRo, cruise, ferries (and yachts) have remained stable and tend to increase. The offshore oil and gas sector has suffered from low oil prices. Spending by oil companies is estimated to have dropped 35% since the end of 2013, but new sectors like offshore wind, marine renewable energies, aquafarming and deep-sea mining are increasing as well as specialized vessels for arctic operation. Even though currently niche markets, this market segments may grow further in the future.

New orders in 2017 are likely to be on par or slightly more than in 2016, given the general poor freight markets; the increased difficulty in arranging debt financing and also raising equity; the consolidation through take-overs or alliances; the prevailing price gap between newbuilding and second-hand tonnage (BRGS Group, 2017). The expansion of the Panama Canal completed in 2016 could encourage new types of ships. Shipbuilding may also be influenced by a predicted increase (by IMF) in global exports from 2.2 % 2016 to 3.5 % (Braura and Mittal, 2017). Also for tankers and LNG there seems to be an increase in demand.

There is a pressure from international and national authorities, banks and creditors, ship owners and shipyards to consolidate and reduce, in an organized way, the worldwide shipping and shipbuilding capacity. For 2016 a decline in shipbuilding capacity is seen, with more than 15

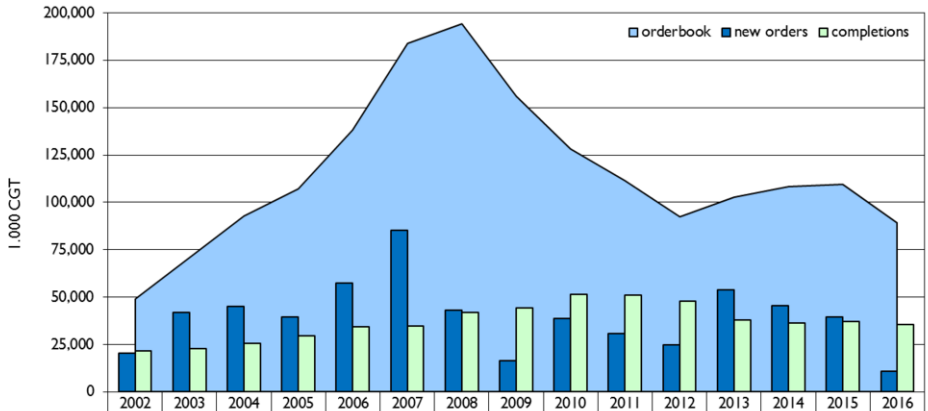


| | 2002 | 2003 | 2004 | 2005 | 2006 | 2007 | 2008 | 2009 | 2010 | 2011 | 2012 | 2013 | 2014 | 2015 | 2016 |
|---|---|---|---|---|---|---|---|---|---|---|---|---|---|---|---|
| orderbook | 48,946 | 70,807 | 92,800 | 107,20 | 138,00 | 183,74 | 194,16 | 156,20 | 128,01 | 111,44 | 92,300 | 102,90 | 108,14 | 109,66 | 89,208 |
| new orders | 20,471 | 41,705 | 45,128 | 39,588 | 57,315 | 85,277 | 42,953 | 16,554 | 38,581 | 30,823 | 24,713 | 53,839 | 45,592 | 39,644 | 10,689 |
| completions | 21,396 | 22,824 | 25,461 | 29,353 | 34,123 | 34,640 | 41,873 | 44,401 | 51,573 | 51,126 | 47,967 | 38,068 | 36,450 | 37,025 | 35,336 |

Figure. 1: Global commercial shipbuilding activity in CGT for the years 2002- 2016. From SEA Europe (2017), data source IHS Fairplay.

Table 1: New orders for different ship categories for the years 2006 – 2016 in M Dwt. From BRS Group (2017).

| New Orders 2006 - 2016 | | | | | | | | | | | |
|---|---|---|---|---|---|---|---|---|---|---|---|
| **M Dwt** | 2006 | 2007 | 2008 | 2009 | 2010 | 2011 | 2012 | 2013 | 2014 | 2015 | 2016 |
| **Tanker** | 77,6 | 48,5 | 35,8 | 8,9 | 29,4 | 8,6 | 13,1 | 33,4 | 32,8 | 48,9 | 13,2 |
| **Bulk** | 47,6 | 142,9 | 85,4 | 23,4 | 88,4 | 39,6 | 24,0 | 75,6 | 58,1 | 24,5 | 15,5 |
| **Container** | 19,2 | 35,4 | 11,6 | 0,3 | 7,3 | 20,7 | 3,5 | 22,5 | 12,8 | 26,9 | 3,3 |
| **Other ships** | 10,4 | 14,3 | 6,3 | 1,3 | 4,4 | 6,7 | 5,9 | 8,7 | 12,3 | 7,4 | 2,0 |
| **Total** | 154,8 | 241,1 | 139,1 | 33,9 | 129,5 | 75,6 | 46,5 | 140,2 | 116,0 | 107,7 | 34,0 |

| Orders for specialised vessels 2009 - 2016 | | | | | | | | |
|---|---|---|---|---|---|---|---|---|
| | 2009 | 2010 | 2011 | 2012 | 2013 | 2014 | 2015 | 2016 |
| **Chemical carriers stainless steel (k Dwt)** | 137 | 265 | 202 | 370 | 939 | 2207 | 2138 | 737 |
| **LPG carriers (k cbm)** | 76 | 933 | 692 | 1424 | 5095 | 5360 | 5121 | 200 |
| **LNG carriers (k cbm)** | 313 | 2262 | 7875 | 6294 | 5531 | 11857 | 4090 | 1078 |
| **Ferries and Ro-pax (k gt)** | 124 | 568 | 57 | 214 | 183 | 299 | 301 | 559 |
| **Ro-ro (k Dwt)** | 198 | 41 | 246 | 659 | 152 | 41 | 151 | 284 |
| **Car carriers (k cars)** | 2 | 133 | 58 | 193 | 288 | 168 | 447 | - |
| **Cruise vessels (k gt)** | 130 | 1069 | 819 | 1510 | 733 | 2241 | 2485 | 1864 |

liquidations in 2016 compared to a few in 2015, and also a very low vessel ordering capacity. The decline in shipbuilding capacity can be exemplified as a change from an estimated 1,150 active yards in 2000 to around 630 yards in 2016, which represents a 35% decline to an estimated 45 million Compensated Gross Tons (CGT). The trend continues with an estimated 3 million CGT set to disappear in 2017. This development has also changed the focus of shipbuilding activities in the world. Thus, many countries and regions aim to enter new market segments of complex high-technology ships and initiated corresponding long-term research and development initiatives (Chen, 2014). This includes developments of new materials and production techniques, e.g. for lighter ships (composite materials), reduced drag and resistance (coatings and air lubrication), retrofitting (e.g. propulsion improvement devices, exhaust gas treatment) and new fuels (gas and methanol). On the legislative side new clean water ballast restrictions coming into force, new Sulphur Emission Control Area (SECA) zones and navigational speed may also push for a replacement and renewal of the fleet.

Table 2 visualizes the market focus, in terms of ship production and orders, as expressed by the different countries and regions. The Table is in a sense relative, but it shows also the dominance of China in the first three categories, where China managed to obtain half the new orders 2016. The Table also shows Korea's strong position in orders for LNG carriers and the strong focus in Europe on cruise, ferries and mega yachts.

Table 2: Activities in ship production and orders in different in different countries and regions. • = some activity, •• =considerable activity.

| Type of Ships | China | Korea | Japan | Europe | Brasil | AUS | US |
|---|---|---|---|---|---|---|---|
| Crude oil tankers | •• | •• | • | | | | |
| Bulk carriers | •• | | • | | | | |
| Product & chemical tankers | •• | •• | • | | | | |
| LNG and LPG carriers | • | • | • | | | | • |
| Container vessels | •• | • | | | | | |
| RoRo and other cargo | •• | | • | | | | • |
| Cruise, PAX and ferries | • | | • | •• | | •• | |
| Mega Yachts | • | | | •• | | • | |
| Offshore vessels | •• | | | | •• | | |
| Naval vessels | | | | • | | •• | •• |

### *2.1 Ongoing research programmes on materials and fabrication technology*

#### *2.1.1 China*

Besides projects funded by the National Natural Science Foundation, there are strong research activities at several universities, on materials for ship and offshore structures (for wind energy, renewable energy, aquafarming and deep sea mining), on welding methods including laser welding and underwater welding, and on controlling distortions during welding.

#### *2.1.2 Europe*

Public funding of maritime R&D projects in Europe comes primarily from the member states and the European Union. Some European countries like Germany have own national maritime research funding schemes, while others fund maritime research through generic programs. The MARTEC II network has analyzed maritime R&D funding programs in the different countries (MARTEC II, 2017). On the European level, research is funded through the Framework Programs, such as FP7 (2007-2013, ca. 50 billion €) and HORIZON 2020 (2014-2020, estimated budget ca. 80 billion €). Maritime projects in HORIZON 2020 are primarily funded under the priorities of Transport (under Mobility for Growth) and Blue Growth (under Societal Challenge 2). Horizon 2020 aim at encourage innovation at higher Technology Readiness levels (TRL) and also include specific funding instruments for small and medium enterprises (SME:s), all aiming to promote the market uptake of research results and industrial competitiveness.

The following list gives an overview on some important maritime projects with relevance to materials and fabrication which were or are active in the period between 2015 and 2018 (European Commission, 2017).

| Acronym | Title |
|---|---|
| HILDA | High Integrity Low Distortion Assembly (friction stir welding) |
| CARLOS | CooperAtive Robot for Large Spaces manufacturing |
| ADAM4EVE | Adaptive and Smart Materials and Structures for more efficient vessels |
| MOSAIC | Materials Onboard: Steel Advancements and Integrated Composites |
| LEAF | Low Emission Anti Fouling |
| SMARTYards | Developing Smart Technologies for productivity Improvement of European Small and Medium Sized Shipyards |
| HOLISHIP | Holistic Optimisation of Ship Design and Operation for Life cycle |
| SHIPLYS | Ship Life Cycle Software Solutions |
| RAMSSES | Realisation and Demonstration of Advanced Material Solutions for Sustainable and Efficient Ships |
| FIBRESHIP | Integral Composite Ship |
| SHIPTEST | Fully Automated Laser Guided Inspection Robot for Weld Defect Detection on Ship Hulls |

Beside the large programs, there is an intense network activity between European companies (with increasing numbers of SME:s) , research institutes and academia, often financed by EU, it stretches beyond research into regulations and commercial activities. One example of such a network is E-LASS an European network fort lightweight applications at sea (www.e-lass.eu).

#### *2.1.3 Australia*

The main source of R&D funding for maritime in Australia is related to Defense and the Federal Government's Australian Continuous Shipbuilding Plan. Two new sources of funding have been provided through The Defense Innovation Hub investing $640 million over the decade in maturing and further developing technologies.

The future Frigate program is developing technologies in the areas of welding and joining, additive manufacturing, corrosion coatings and corrosion prognostic health monitoring, single crystal sonar ceramics, toughened composites and blast and shock modelling software tools. navigational speed may also push for a replacement and renewal of the fleet.

Table 3 visualizes research efforts in materials and fabrication technology as expressed by the different countries and regions. Steels, and welding methods still have strong position in several countries and regions, though research on non-metallic materials, eg composites and also additive materials and ICT / digitalization are emerging areas.

## 3. MATERIALS

### *3.1 Low temperature steels*

Recent efforts to avoid the serious environmental pollution reinforced the International Maritime Organization (IMO) regulations for nitrogen oxide (NOx). In particular, the Marine Environmental Protection Committee (MEPC) of the IMO agreed upon progressively stricter limitations for NOx emissions from ocean going vessels (Azzara et al., 2014). In this trend, various types of LNG carriers such as liquefied natural gas carriers (LNGC), floating liquefied natural gas (FLNG), LNG-floating storage regasification unit (LNG-FSRU) and very large gas carrier (VLGC) have been developed and are currently operating worldwide.

Table 3: Research efforts in different countries and regions.
• = some activity, •• =considerable activity.

| Research projects / programs | China | Korea | Japan | Europe | Brasil | AUS | US |
|---|---|---|---|---|---|---|---|
| **Materials** | | | | | | | |
| Steels | • | •• | •• | • | •• | •• | • |
| Other metallic materials | • | •• | | | • | • | •• |
| Non-metallic materials | • | • | • | •• | •• | • | • |
| Coatings | • | • | | •• | | • | |
| **Fabrication and joining** | | | | | | | |
| Welding | •• | • | •• | • | •• | •• | •• |
| Adhesive bonding | • | • | | •• | | • | |
| Automation | •• | • | • | • | • | • | • |
| Additive materials | • | • | •• | • | •• | • | • |
| Qualitative control and management | • | • | | •• | •• | | |
| ICT, digitalization | •• | • | •• | •• | • | | |

One of the most important issues in the design of LNG carriers is the structural integrity of storage tanks under cryogenic temperature. Therefore, LNG storage tanks are typically manufactured using low temperature steels considering the operation temperature of LNG. In terms of the structural integrity of storage tanks, researches of low temperature steels mainly have focused on fatigue and fracture performances at cryogenic temperature. Also, further research of high manganese steel is being carried out to register the steel in International Gas Carrier (IGC) code. The most common low temperature steels are:

- Nickel steels (The contents of 3.5%, 5%, 7%, 9% nickel)
- Stainless steel (SUS 304L, SUS316L)
- Aluminum alloy (Al 5083-O)
- High manganese steel

### *3.1.1 Nickel steels*

Nickel is one of the most utilized and important major industrial metals. In particular, nickel-iron alloys are commonly used in demanding corrosion-resistant and heat-resistant applications. Therefore, nickel steels have been used mainly for the primary barrier of LNG storage tanks. In this respect, some researches have been carried out to assess the fatigue and fracture performances of nickel steel. Pusan National University (PNU), Hanjin Heavy Industry and POSCO (2016) studied material characteristics of 9% nickel such as material properties, fatigue and fracture performances for the application of IMO Type C LNG Cargo Containment System (CCS). They performed tensile, Fatigue Crack Growth Rate (FCGR) and fracture toughness tests considering three different welding consumables and two welding processes. Scheid et al. (2016) assessed fracture toughness of 5.5% and 9% nickel steels regarding the effect of heat treatment. In addition, Park et al. (2016) evaluated material characteristics of 3.5 to 9 wt% nickel steels. Fatigue Ductile to Brittle Transition (FDBT) phenomenon was investigated to determine the requirement of classification. In addition, the fatigue and fracture performances are compared among 3.5% to 9 wt% nickel steels for both room and cryogenic temperatures. In order to find the suitable FCGR design curve, material constants of nickel steels are compared with the value in BS 7910 standard.

#### *3.1.2 Stainless steels and aluminum*

Stainless steels and aluminum are being considered as possible material candidates for primary barrier in IMO Type-B tank. In order to ensure the structural integrity of such tanks, it is very important to evaluate the fatigue and fracture performances at cryogenic temperature. Kumar et al. (2016) investigated impact toughness behavior at Heat Affected Zone (HAZ) and weld metal considering three different heat inputs as well as two thermal aging conditions. This study conducted Charpy V-notch (CVN) test at room and cryogenic temperatures. Chaves et al. (2017) evaluated fatigue limits for SUS and Aluminum from pure tension to pure torsion. In this study, the geometry of specimen is a thin-walled tube with a passing-through hole. Jesus et al. (2016) assessed the influence of Friction Stir Processing (FSP) on the fatigue behavior of Gas Metal Arc Welding (GMAW) T-welds in AA 5083-H111 plates. As a result, the fatigue strength of GMAW T-welds is found to be significantly improved. Ilman et al. (2016) investigated improving fatigue performance in AA 5083 metal inert gas (MIG) welded joints through mitigated distortion and residual stress using static thermal tensioning (STT).

#### *3.1.3 High manganese steel*

The increasing demand for strong and tough steels for cryogenic applications leads to the development of high-Mn austenitic steels utilizing Twining Induced Plasticity (TWIP) effect. Song et al. (2016a) performed to clarify the effect of Al addition on Low-Cycle Fatigue (LCF) properties of high - Mn TWIP steels, which were electro chemically charged by hydrogen. In addition, Song et al. (2016b) investigated the effect of cold-drawing on the fatigue properties of austenitic TWIP steels, and the results were compared with those of conventional Fully Pearlitic (FP) steel. Jeong et al. (2016) evaluated the FCGR behavior of high-Mn steels with a variety of chemical compositions in order to understand the controlling factors determining the near-threshold characteristics of crack propagation.

### *3.2 High strength steels*

Many researches have been carried out to assess the fatigue and fracture performances of high strength steels. It is well known that the interior of a thick plate is in a plane strain state with the plastic region decreased in size (Kaneko et al., 2011). As a result, a stress greater than its yield stress is generated, and fatigue and fracture performances significantly decrease. The main topics of high strength steel are brittle crack arrest and improvement of fatigue strength. An et al. (2014) investigated brittle crack arrest fracture toughness with a high heat-input welding. Hase et al. (2014) developed a heavy thick YP460 steel plate with excellent brittle crack arrestability for the upper deck and hatch side coaming areas in mega container carriers. The fatigue strength improvement as a function of the yield strength was observed also for post-weld treated joints in Yildirim and Marquis (2012). Laitinen et al. (2013) showed that an increased fatigue strength can be obtained for cut plate edges without treatment, when cutting quality is good.

Recently, ultra large container ship that can carry more than about 20,000 TEU are being constructed. According to this trend, ships and offshore structures are under more demands for thicker plates to ensure the sufficient strength. In the case of large container ships (above 12,000 TEU), in particular, the high strength steels with a thickness of 80 mm are commonly applied to the hatch coaming section.

Liu et al. (2016) evaluated the effect of step quenching on microstructures and mechanical properties of High Strength Low Alloy (HSLA). Shibanuma et al. (2016) proposed a new model formulation to predict brittle crack propagation and arrest behaviors. Usami et al. (2016) reported the process and results of a risk analysis of cryogenic fluid leaks as well as the study on a prospective measure to mitigate the risk by use of a newly developed TMCP steel having brittle fracture arrestability. Kumar et al. (2016) investigated Ductile to Brittle Transition Temperature (DBTT) for HY 85 steel which is a high strength low alloy steel used in the

quenched and tempered condition specially developed for ship hulls. Lan et al. (2016) evaluated the impact toughness of HSLA steel with multi-pass Submerged Arc Welding (SAW). The effect of hydrogen on the fracture and impact toughness of ultra-high-strength steels at sub-zero temperatures were investigated by Pallaspuro et al. (2017). The influence of welding thermal cycles produced by reheating processing on mechanical properties was evaluated by Wang et al. (2017).

Shiozaki et al. (2015) assessed the relationship between residual stress and fatigue strength for as-punched specimens and specimens subjected to stress relief heat treatment after punching a hole. Mora et al. (2015) focused on the effect of sea water corrosion on the Giga-cycle fatigue strength of a martensitic–bainitic hot rolled steel R5 used for manufacturing off-shore mooring chains for petroleum platforms in the North Sea. Harati et al. (2015) compared the fatigue strength of as welded with that of High Frequency Mechanical Impact (HFMI) treated fillet welds in a 1300 MPa yield strength steel. Ottersböck et al. (2016) investigated the effect of single undercuts as characteristic weld defects on the fatigue behavior of high quality ultra-high-strength steel welds. The fatigue strength of TIG-dressed Ultra High Strength Steel (UHSS) fillet weld joints at different stress ratios was determined by experimental testing, and a statistical analysis was applied to local geometric factors and variables of manually TIG-dressed fillet welds (Mikkola et al., 2016). Harati et al., (2017) evaluated residual stress and fatigue strength of high strength steel welded joint considering difference in four Low Transformation Temperature (LTT) welding consumables. Leitner et al. (2017) contributed to quantify the influence of the local mean stress condition and the local weld geometry on the high-cycle fatigue strength of welded and high frequency mechanical impact (HFMI) treated S960 high-strength steel joints.

### *3.3 Steels for use in the arctic*

It is well known that when the temperature decreases, steel becomes more brittle. In addition, the yield and tensile stress increase with decreasing temperature (Østby et. al. 2015) and the detailed shape of the stress-strain curve may change, e.g. the length of possible Lüders plateau may change (will elongate with lower temperatures). The benefit of an increased yield strength is not considered in design in the offshore and maritime industry today.

A structure or component need adequate toughness for the loading seen at low temperatures to prevent brittle fracture in the Arctic. None of the common offshore design codes today consistently addresses low temperature applications; EN 10225 is applied down to -10°C, NORSOK specifies a lower bound design temperature of -14°C while ISO 19902 does not state a lower bound of the design temperature and operate with requirement to material testing at lowest anticipated service temperature (LAST). ISO 19906 “Arctic Offshore Structures” requires that the Design Class (DC) approach in ISO 19902 shall be applied, which for the highest toughness class of materials requires steel to be tested 30 °C below LAST. Hence, for a design temperature of -40ºC would then typically require Charpy testing at -70ºC. Both Norsok and DC in ISO 19902 specify material per EN 10225 where Charpy testing at -40°C is the lowest test temperature required. It can be noted that EN 10225 currently are under revision with an aim to include materials for arctic offshore application. There is also an ISO working group, ISO TC67/SC8/WG5, drawing up standardized material requirements for Arctic Operations (Hauge et. al 2015). The committee has representatives from Russia, Canada, the Netherlands, Italy, France, Germany and Norway.

“Recognized Class Societies” (RCS) defines the temperature to be used for material selection to be based on the lowest Mean Daily Average Temperature (LMDAT). This temperature is used for structural material selection and should be based on several years of observations. While ISO 19906 for Arctic offshore structure defines the lowest anticipated service temperature (LAST) as the minimum hourly average temperature with a return period of 100

years. ISO 19904-1 opens for either using the LAST or LMDAT (RCS approach) for setting the material temperature.

Setting the material test temperature based on LAST or MDAT provide large difference as shown for a location in the Barents Sea, see Figure 2, where LMDAT gives a temperature of -7°C and -30°C for LAST respectively (Horn et al., 2016).

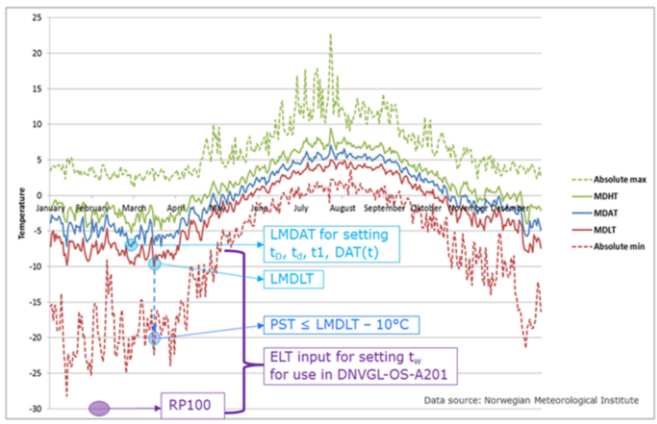


Figure 2: Temperature observations at Bjørnøya from 1998 to 2012. From Horn et al. (2016).

In general, ship and vessels are built to a fixed temperature, which often is set to -10ºC regardless of the location, transport rut etc., except for polar vessels, which are regulated under SOLAS and MARPOL. The same goes for jack-ups which in many cases are specified for -10ºC or for some extreme cases down to -20ºC. These design temperatures are in line with the -10 to -14ºC "qualification of steel materials in Offshore" per EN 10225 and Norsok M-101.

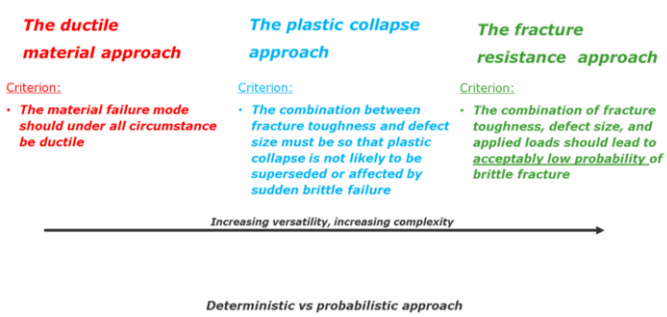


Figure 3: Material approaches. From Østby et al. (2015).

For lower temperatures than -10ºC it is up to the designer to demonstrate adequate toughness at lower temperature, some guidance can be found in Østby et al. (2015) and Horn et al. (2016) and is shown in Figure 3.

Today, it is common to test fracture toughness (CTOD) for the actual design temperature regardless of the utilization at the minimum design temperature. Horn et al. (2017) discuss the toughness in relation to CTOD and thickness and temperature effect. Based on the assumption of absolute stress level controlling the initiation of brittle fracture and an empirical representation of the yield stress dependence on temperature which increases at low temperature, a simplified scheme to transfer toughness levels between different temperatures has been discussed and compared with e.g. the master curve, see Figure 4. The proposed scheme

may have application when having to considered design scenarios with different temperatures, like transportation, installation and operation.

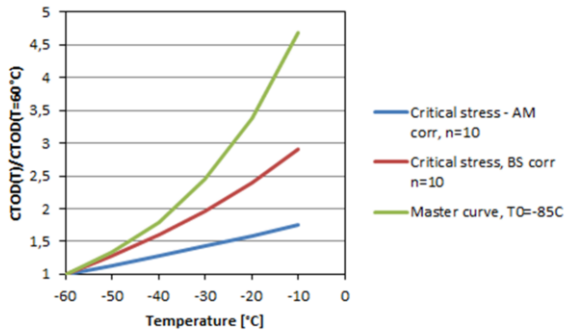


Figure 4: Comparisons of relative critical CTOD as a function of temperature using different models/assumptions. From Horn et al. (2017).

There is currently a focus towards materials behavior under Arctic conditions like the Arctic Materials project managed by SINTEF (2008-2017) (Akselsen at al., 2017). The research project has shown that good toughness values can be demonstrated by the base material, however generally the HAZ and weld metal show lower toughness values, especially in inter critical region in the HAZ, Østby et al (2014). Large scatter in the toughness results have been seen for low temperature toughness testing, (Akselsen et al., 2017) and in Østby et al. (2015) when more than 10 CTOD tests are run. In the Arctic Material project guidance toughness criteria given as CTOD values have been proposed by Østby et al. (2015). In Figure 5, the effect of temperature on toughness is shown for the two different weld thermal simulated

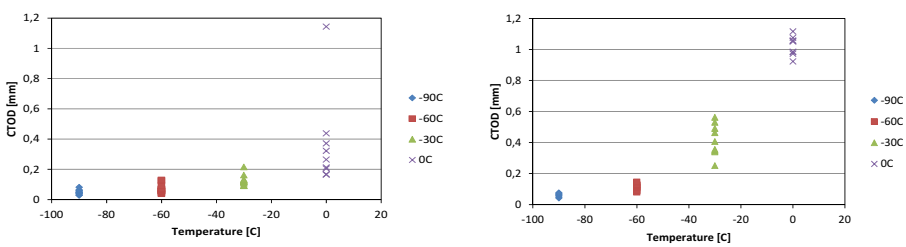


(a) (b)

Figure 5: CTOD values as function of temperature. a) CGHAZ (b) ICCGHAZ. From Østby et al. (2013).

HAZ microstructures CGHAZ and ICCGHAZ. As expected, the fracture toughness increases with increasing temperature (Østby et al., 2013).

Vessels that intend to operate within the Arctic and Antarctic areas as defined in the Polar Code need to comply with the Polar Code which entered force on 1 January 2017. For ship structures intended to operate in low air temperature, materials used shall be suitable for operation at the ships polar service temperature. The Polar Code refers to IACS UR S6 Use of Steel Grades for Various Hull Members – Ships of 90 m in Length and Above (latest version) or IACS URI Requirements concerning Polar Class (latest version), as applicable. IACS UR S6.3 has selection criteria for minimum steel grade requirements of ships operating in low air temperature environments. Based on the ship's design temperature, a structural member's

thickness and material category (i.e., criticality), minimum steel grades are prescribed. The most stringent material quality is use of F class for $35 \leq t \leq 50$ for PC1-3 (most stringent is PC 1 with Year-round operation in all polar waters).

### *3.4 Composite materials*

Marine composites are typically constituted by multi-layered laminates, where each ply can be represented by an orthotropic layer. An orthotropic material admits three symmetry planes; thus, the resulting elastic matrix is defined by 9 independent elastic constants in 3 space, and by 4 elastic constants considering a plane stress condition, which is often the case for marine structures applications, characterized by relatively small thicknesses if compared to other dimensions.

The typical fiber reinforced composite is constituted by a polymeric matrix, which cures on the reinforcing fibers on a mold. The fibers sustain the load, in terms of stress, and provide the stiffness; moreover, the fibers also act as crack stopper limiting the fracture propagation, originating both in the matrix and in the fiber.

On the other hand, the matrix equally distributes the loads among fibers and provide the inter-laminar shear strength. Its tasks are also to resist against chemical aggressions and to allow an ultimate deformation higher than the one of fibers, to prevent from matrix failure at low fiber stress.

In the following, some peculiars aspects are considered resulting from the literature review of the last three years. Earlier findings and general descriptions may be found in Tsai and Hahn (1980), Shenoi and Wellicome (1993) and Jones (1998).

#### *3.4.1 Mechanical aspects*

The micro-mechanics considers the interaction between fiber and matrix in the isolated ply, assumed as linear-elastic orthotropic, and defines the elastic constants derived from analytical formulations or, when available, from experiments. Analytical formulations like the so called “mixture rule” are well-established and provide reliable results in terms of axial modulus and in-plane Poisson coefficients, starting from fiber and matrix properties. On the other hand, empirical corrections derived from experimental campaigns are still necessary to overcame limits originating from simplified assumptions in order to define the remaining elastic constants. Among the others, the Halpin-Tsai correction is still likely the most popular in current literature (Halpin and Kardos 1976).

More difficult is to predict reliable data for the strength of the lamina, as the manufacturing process has a strong impact on such parameters and composites obtained from very same fibers and matrix can show completely different behaviors. Manufacturing imperfections, like air inclusions, de-cohesions and fiber misalignment, and chemical features, i.e. the influence of ambient and laminate temperature while curing and humidity, may seriously affect the composite strength as well as its failure modes. This aspect is widely covered in literature, and confirmed in recent works by Godani et al. (2014), Kim et al. (2014), Kalantari and Dong (2017), in addition to earlier references.

The macro-mechanics allows the prediction of the laminate response when subjected to forces and moments, and is based on the so-called “Classic Laminate Theory”, which linearly adds the contribution of each ply to obtain the global stiffness of the composite laminate, given its stacking sequence. The theory is well established and implemented by most of the commercial finite element software when modelling multi-layered composites: it provides reliable results within the material elastic range of each ply. In practice, the mid-plane strains are calculated, as well as the laminate curvatures, from equilibrium considerations. A thru thickness linear variation of strain is assumed and the stresses are computed at each ply. Different failure models can be adopted to asses for the ply failure: the most commonly adopted currently by leisure

boat industry is the maximum strain failure criterion. Other criteria include maximum stress, Tsai-Hill, Tsai Wu and their derivations.

Nonlinear response associated to material failure still represent a challenging task for composite materials. In order to predict the post first ply failure and collapse behavior, orthotropic "plastic" models, with a close to zero admissible plastic deformation, were successfully adopted by Maggiani et al. (2017).

It is worth noting that composite materials present a number of failure modes, which is much higher if compared to traditional isotropic ductile materials, and current theories only provide reliable results to asses for the first ply failure only of laminates: among failure modes, the most critical to assess is the delamination.

Relevant works were conducted in recent years to predict the opening and the growth of delaminations in fiber-reinforced composites, and to assess for their effect in terms of global response of the structure. Gaiotti et al. (2014) compared different numerical strategies to determine the buckling capacity of delaminated composite panels and Colombo and Vergani (2014) studied the effect of delamination on fatigue behavior. Considering the advances of numerical simulations in this field, although the theory was developed in the past decades, due to the high computational efforts cohesive elements have become available in finite element software only recently. This fact has introduced a new tool to simulate delamination opening and growth; by the way, current applications only limits to small-scale models because of two main reasons, both related to computational limits: primarily because of the higher number of elements required to simulate cohesive layers, and secondarily since cohesive are solid elements requiring a 3D-solid modelling strategy.

In general, cohesive models currently represent a powerful instrument to investigate the influence of cohesive parameters in small scale model, while their implementation in large scale design is still far from being achieved due to computational limits. Some promising applications include the analysis of local problems, as well as the numerical characterization of the material capacity to resist against delaminating stresses as reported by Cricrì and Perrella (2016) and Woo et al. (2017).

### *3.4.2 Recent technological innovations*

Another innovation related to reinforcing fiber were led by the introduction of the stitched fibers or non-crimp fabrics that are able to maintain the planarity of the reinforcement. The benefit of non-crimp fabrics leads to an increment of the tensile strength of about 20 to 30 %, being equal the glass content with respect to a woven fabric, according to an investigation conducted by the author upon reinforcements currently available on the market. Moreover, the lower number of interstitial space between non-crimp fibers also allows an increment in the composite fiber content, leading to a further improvement in terms of material properties. On the other hand, non-crimp fibers are more expensive than traditional woven roving, thus their application is limited to high performance composites. Another critical aspect was highlighted by Shiino et al. (2017) in delamination problems, which found a decrease in the surface propagation energy because the stitch yarn replaced the carbon fiber/epoxy interface, which has better chemical affinities

### *3.4.3 Composites for subsea applications*

Composite risers are expected to be a high-impact technology that will be mainstream in the medium term. Nevertheless, due to the complex behavior and damage mechanisms presented by composite materials, when compared to metallic materials, the use of composite risers represents new challenges in terms of design and analysis procedures. There are still few references addressing the behavior of these composite risers in deep water. Pham et al. (2015) presents a comprehensive literature review on manufacture, testing and numerical simulations

of composite risers in deep water conditions, indicating some of the gaps and key challenges for their near future application growth.

FRP composites offer good potential for the design of deep-water risers. Thermoplastic composite risers (TPCR) offer good solutions to current limited technologies in metal Top Tensioned Risers (TTRs) and Steel Catenary Risers (SCRs), related to high costs for buoyancy and compensation system used to support their own weights at deep-waters. Composite risers demand lower top-tension and less or even no buoyancy, leading to a significant weight hanging reduction from the platform deck, this is economically beneficial which increase with increasing length. Furthermore, the size of the tensioner joint and tapered stress joint needed at the top and bottom of the composite riser system are considerably smaller than that of the steel riser system.

When compared to steel risers, composite risers have shown better resistance against many failure modes, including burst, collapse, leakage and crack through the liner and composite tube. Tan et al. (2015) stated that composite risers are more vulnerable to vortex-induced-vibrations (VIV), and therefore fatigue damage, than steel risers. This strength deterioration arises from a temperature increase, which is worst for deeper reservoirs. These effects can be avoided by increasing the fiber-winding angle, increasing the load bearing properties and raising eigenfrequencies, mitigating the VIV. Chen et al. (2013) found that the high stiffness of the liner reduces the overall performance the composite riser under VIV, as the high strength of the composite cannot be fully utilized.

Tan et al. (2015) carried out full-scale study experiments and numerical simulations aiming to compare steel risers and composite risers (with aluminum, steel and titanium liners). The results showed the liner is the weakest link for composite riser design. The titanium liner riser yielded 20% lower RMS strains than the aluminum liner riser and 10% lower RMS stress than the steel liner riser. It was then concluded that titanium alloys are a better choice than steel due to their density, wear and corrosion resistance.

Moreover, composite risers can be classified into two main types: bonded and unbonded. In the first type, the riser's layers are bonded, while in the second type, the relative movements between riser's components are not restrained. Bonded risers often include a core fiber-reinforced angle ply laminate sandwiched between an inner liner of metallic/elastomeric material and an outer liner of thermoplastic/ thermoset material or metal alloy, with the primary role of the liners being to prevent weeping and fluid leakage. DNV-OSS-302 (Det Norske Veritas, 2010) gives detailed design criteria for bonded FRP risers.

The metal-to-composite interface (MCI) is mainly used to provide an adequate contact between the composite pipe body and the metallic end fittings at pipe's terminations, which helps to effectively transfer loads between the pipes. An efficient design of the MCI is important since their length and mass may significantly affect the weight-effective use of composite risers and failure often occurs at this point. Efficient designs for end fitting are crucial for minimizing damage at the MCI, as well as guarantee good load transferring between the composite tube and metal components.

### *3.5 Weight reducing materials*

The weight reduction we typically associate with replacing traditional materials with composites has different implications for ships. For military customers, the potential to incorporate smart functionality and reduce magnetic, radar and infra-red signatures is an obvious advantage. Composites are already used in military ships in several applications including: superstructure, masks, radomes, hangar and so on. However, it is noticed that composites are usually applied in non-main component in ships. One did not see a larger fighting naval vessel after Swedish Visby.

Composites are already used in commercial ships in several applications including: masts and radomes, lifeboats, pipework. Complete composite valve and pipework systems are available which have a major benefit in terms of corrosion resistance for seawater cooling systems. In commercial ships, taking account of the high cost, composites have not large-scale used. Recently, the concept of composite hatch, which was developed by Oshima Shipyard, has been raised. These bulk carrier hatch covers are 17 m by 8 m for each half and would weigh 36 tonnes in steel, but just 12 tonnes in GRP. Most of the top reasons for insurance claims for damage to cargo are related to hatch covers-problems with seals, corrosion, etc. The GRP covers would reduce many of these problems, and allow for smaller electric motors and lighter craneage.

A huge problem in steel ships is corrosion in ballast tanks. The tanks are integral to the structure of the hull, so structural beams pass through them, creating complex surfaces that are very difficult to maintain. A fully composite structure could solve this problem, but to suggest a composite hull for a large ship is a big step from where we are now. Because of its advantage in weight reduction, composites were applied in submersible vehicles. American 'Alvin', French 'Nautile' and Japanese 'Shinkai' manned submersible adopt composite to their outer hull shell. Outer hull shell doesn't bear huge underwater pressure and its major function is keeping structure outer shape to improve hydrodynamics performance and protect inter equipment. As composites low density and high strength advantage, it almost fits all of requirement of submersible vehicle outer hull shell.

Properties of cast aluminum components can be improved by strategically placing ferrous inserts to locally improve properties such as wear resistance and stiffness. A cost-effective production method is to cast-in the insert using the solidification of the molten aluminum as a joining method. Metallurgical bonding between the metals could potentially improve both load and heat transfer across the interface. The metallurgical bond between the steel and the aluminum has to be strong enough to withstand stresses related to solidification, residual stresses, thermal expansion stresses, and all other stresses coupled with the use of the component. Formation of a continuous defect free bond is inhibited by the wetting behavior of aluminum and is governed by a diffusion process which requires both energy and time. Due to the diffusional nature of the bond growth in combination with post manufacturing heat treatments defects such as Kirkendall voids can form.

The effect of aluminum alloying elements during liquid-solid bond formation in regards to microstructural changes and growth kinetics has been described (Soderhjelm and Apelian 2016). A timeframe for defect formation during heat treatments as well as microstructural changes has been established. The effect of low melting point coatings (zinc and tin) on the nucleation of the metallurgical bond has been studied as well the use of a titanium coating for microstructural modification. A set of guidelines for successful metallurgical bonding during multi-material metal casting has also been constructed.

In another research effort relating to light-weighting, aluminum based nano-composites containing, AlN, TiC, SiC and $Si_3N_2$ second-phase has been studied as an alternative for higher impact and fatigue strength material for structural applications (Udvardy, et.al. 2012).

## 4. JOINING AND FABRICATION

With certification and qualification of welds being a fundamental input for ship structural integrity, shipbuilders have generally persisted with the classic joining technologies as a proven fabrication option. But as ship designers more commonly use higher strength steels with thinner panels to lighten ship's hulls, distortion becomes a prominent issue for both assembly and ship operations, and so new advances in low heat input welding and joining technology need to be considered.

### *4.1 Advances in joining technology*

There are three key areas shipbuilders use to control distortion: 1) during the design phase where increased stiffness and steel choices affect rigidity, 2) during the welding and joining process itself, and 3) through costly rework to correct distortion after it has occurred. When considering the joining process, the ability to either lower the heat input and/or carefully control the distribution of heat, has the potential to reduce residual stresses remaining after the assembly process.

#### *4.1.1 Low heat input welding processes*

In recent years, there are several low heat input processes which have been studied and/or made commercially available as an alternative to the higher heat input process Submerged Arc Welding (SAW). Some of these include Double Electrode (DE-GMAW), Tandem welding (T-GMAW), Double Sided processes (DSAW), Plasma Arc Welding (PAW), Keyhole TIG welding (K-TIG), Laser Beam Welding (LBW), Laser Hybrid welding (HL-GMAW) and Friction Stir Welding (FSW). However, the latter three will not be discussed, since these processes have been covered in previous report.

Tandem processes, on the other hand, include any process that duplicates the number of wire fed electrode and thus the deposition rate. Like hybrid laser or double electrode processes, several variants of the tandem process exist. The Pulsed Tandem Gas Metal Arc Welding (PT-GMAW) and Tandem Gas Tungsten Arc (T-GTAW) are the main studied processes and are commercially available. For the PT-GMAW, two welding wires are independently controlled wires are fed into the same weld pool. The synchronized pulse and electrically isolated electrodes allows the process to independently alter the leading and trailing wire feed and current/voltage settings. The effect is a controlled distribution of energy within the weld pool which results in lower overall heat input and resultant distortion. Doubling the number of electrodes also allows to reduce the number of passes and thus the production cost. Sproesser et al. (2016) showed that indirect savings are also achieved with a comparison of GMAW and PT-GMAW multi-pass processes on a 30mm 355J2+N butt weld. Besides the 55% reduction of the welding time, a 23% reduction of the electricity consumption and a 5% reduction of the total used filler wire was obtained, making it a more cost-effective and sustainable process (Sproesser et al., 2016).

*Double electrode processes* include any process that uses as second electrode. Generally, a Plasma Arc or GMAW torch is used to bypass some of the current, as shown in Figure 6, resulting in a reduced heat input in the weld pool. It also decouples the deposition rate from the heat input. Estifen et al. (2010) compared DE-GMAW with GMAW on 19 mm butt welds of ASTM 131 grade A shipbuilding ferritic steel and showed a reduction of the number of passes from 11 to 3 and a 40% reduction in the out-of-plane distortion. However, there was no significant reduction in angular distortion.

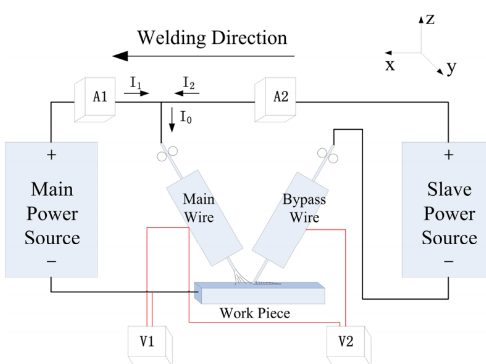


Figure 6: Schematic drawing of the Double Electrode Gas Metal Arc Welding process. From Wei et al. (2015).

The European research fund for coal and steel funded a three year study of the tandem processes (Thompson et al., 2008). Their main conclusion was that tandem processes lead to productivity increase from 50 to 100% without any detrimental effect on fatigue or toughness. They also concluded that T-GMAW was not efficient to reduce buckling distortion in comparison to single

GMAW but was efficient to reduce angular and bending distortion. They produced butt welds, fillet welds, and lap welds for S355 plates varying from 3 to 12 mm thicknesses.

A study and technology implementation by Larkin et al. (2011) showed that when using T-GMAW instead of SAW, angular distortion can be reduced by 60% on a 5mm DH36 single sided butt weld for naval ship panels. Similarly, the out-of-plane longitudinal distortion was reduced by 20% while doubling the welding speed up to 1.4 m/min with a 30% reduction in weight of filler material required (Larkin et. al., 2011). More recent work by Sterjovski et al. (2011) on 8 mm HSLA65 butt weld showed that distortion was reduced by more than 50% in comparison to standard GMAW process (Sterjovski et al., 2011).

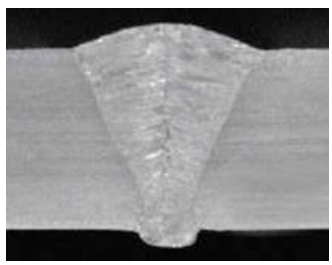

Figure 7: Macrograph of 8mm BW 316Ti Keyhole plasma arc welding. From Knautz (2017).

*Plasma arc welding* (PAW) is very similar to GTAW except that the arc is constricted in a plasma gas making it a very high-density energy process. The plasma gas itself is maintained in a classic inert gas flux. It is useful for welding thick plates with minimal joint preparation due to high-density of the beam. The process is defined as a Keyhole-Plasma Arc Welding (K-PAW) when the plasma jet penetrates completely through the work-piece. Without backing, the plasma can produce a uniform butt weld with a narrow Heat Affected Zone (HAZ) with reduced heat input. In a single pass, it can weld up to 0.5 m/min with a thickness up to 8 mm, as shown in Figure 7.

Double sided arc welding processes differ from tandem processes as the two welding heat sources are on opposite sides with the aim of balancing the heat input (Mochizuki and Toyoda, 2007). Their research investigates the effect of introducing a distance between the two torches. The advantage of having a fore and a rear torch, besides the balancing effect, is to induce a preheating effect (Mochizuki and Toyoda, 2007) like in tandem processes. Angular distortions could be completely removed using optimised welding parameters (Zhang et al., 2008)

Most recent research use two identical torches, whether they are GMAW (Li et al., 2015) or GTAW (Zhang et al., 2008). However, reported welding speeds are quite low in the literature (0.1 to 0.4 m/min) and the double-sided processes seem to have found more interest in thick plates applications. Thicknesses up to 50 mm have been welded using multi-pass DSAW with SAW (Yang et al., 2014) or DSAW with GMAW (Chen et al., 2015).

A similar process is the *Keyhole Tungsten Inert Gas (K-TIG)* welding process*;* although no plasma is required, making it an easier process to implement. According to the manufacturer, the process can weld up to 16mm thick steel plates and weld at 0.75m/min on 4 mm plates. Both PAW and K-TIG offer an alternative to the costlier laser key hole processes.

In summary, the uptake of each of these described low heat input processes within shipbuilding is varied. Besides laser beam welding, there are few instances of alternate low heat input welding methods being routinely used in production. For the Australian and US naval shipbuilding, there are two examples of panel line construction using PT-GMAW, and ongoing research (Leviel et al., 2017) on fillet welds for stiffened panels. For all other processes, production trials are generally the extent of their implementation.

#### *4.1.2 Secondary Processes - Active distortion control*

*Low Stress No Distortion (LSND)* processes use secondary heating or cooling sources to modify the local thermal profile of the resultant weld. These secondary thermal inputs are not used to influence the weld fusion process but instead only to modify the residual stress state and the structure distortion. The first distinction that has to be made within various forms of LSND processes is whether the heating or cooling source is moving or not.

In *Static-Low Stress No Distortion (S-LSND)*, fixed heating and cooling sources are used to balance the thermal profile to impede the plastic strain accumulation during the heating stage of welding and thus the stress formation. To obtain the adequate thermal profile, cooling is applied to the weld zone area. In some applications, the surrounding zone is also heated. A 170˚C difference is sufficient to prevent buckling in 4.8 mm DH36 stiffened panels (Conrardy et al., 2006). With optimised parameters, it can result in very low stress and almost distortion-free samples. However, generating the optimised thermal field evenly on the whole structure requires devices that are industrially impractical, costly and environmentally unfriendly. It is therefore recommend using transient heating discussed later.

A recent application to 3 mm aluminium butt-welded plates was published by Bajpei et al. (2016). They compare the cooling effect of a heat sink backing plate, of compressed air and of atomised water applied to the back of the weld. By using a numerical model validated with residual stress measurements, they show that angular distortion can be reduced by 50% and that shrinkage is almost eliminated.

In contrast to S-LSND, Transient - Low Stress No Distortion (T-LSND) processes use a moving secondary source. They are further categorised between processes using heating sources, known as transient heating and the processes that use a cooling source immediately behind the welding source. Because the heating or cooling sources are moving, the induced mechanisms, stress, and distortions results are completely different to S-LSND. Side heating is one method used, and although it has been shown to be very efficient to reduce buckling distortion (Pazooki et al., 2016), it has some drawbacks that need to be overcome. Because the plates are heated on one surface, the through-thickness thermal gradient is increased which causes more angular distortion. Although it can be controlled through severe clamping, it is unlikely that this solution would be used to weld large structures. Secondly, the reported welding speed in the literature are low (0.27-0.38 m/min). Transient reverse-side heating, or line heating, consist of applying a heat source on the opposite side of the weld. The process is thus very similar to asymmetric double-sided processes except that only one of the two torches is effectively welding. Mochizuki and Toyoda applied reverse side heating to reduce the angular distortion of fillet welds (Mochizuki and Toyoda, 2007). A relatively high welding speed of 1.8 m/min have been reported. The main drawback is that it only corrects the angular distortion.

*Dynamically Controlled Low Stress No Distortion (DC-LSND)* process uses the principle of a welding process trailed by a cooling source to reduce buckling distortion. Rotational distortions in fillet welds, caused by the bending of the plate and the stiffener, can also be reduced (Mochizuki et al., 2006). Several recent studies have used different cooling agents (Sudheesh and Prasad, 2015, Van der Aa, 2007, Okano and Mochizuki, 2016), however, $CO_2$ snow has been widely reported as being the most effective (Shen, 2013, Van der Aa, 2007). The $CO_2$ becomes solid at -78°C producing a snow jet. Part of the efficiency of the $CO_2$ snow as a cooling agent is attributed to its temporary solid state which induces good contact with the weld metal surface (Van der Aa, 2007). However, application of $CO_2$, produces an undesirable effect of disturbing the welding shielding gas flow as result of a turbulent flow of gas/liquid/solid being applied to the metal surface in close proximity to the welding process. For this reason, application with laser welding or FSW is easier. For application with GMAW or GTAW processes, several approaches have been tried to separate the two sources including intermittent welding or shielding as shown in Figure 8 (Holder, 2011, O'Brien et al., 2015 and Nagy, 2012).

Figure 8: Roller with silica based woven textile Refrasil® wool. From Holder (2011).

A study by Price et al. (2004) achieved an 80% reduction of the distortion index (average measured distortion) using $CO_2$ cooling for 5 mm DH36 plates (Price et al., 2004, Nagy, 2012). Nagy's own experiments, which focussed on buckling distortion, adapted a patented vacuum shield. He achieved butt welds on 4 mm DH36 with a 50% reduction of the out-of–plane peak longitudinal distortion when compared to the classic GMAW process. Currently there is no reported manufacturing use of this technology in shipbuilding production.

Table 4 summarises the main features of the different welding processes discussed above for the case of butt welding of DH36 steel. It is seen that the laser beam welding (LBW) gives the thinnest HAZ but also for the highest investment cost. Submerged arc welding (SAW) gives the widest HAZ and also large residual longitudinal stresses.

Table 4: Summary of the main characteristics of welding processes in DH36 butt welds.

| Process | Vickers hardness peak value [kgf/mm2] | Longitudinal residual stress peak value [Mpa] | Typical welding speed [m/min] | Comparative investment cost from low ($) to high ($$$$) | Fusion zone area / Fusion zone area of the SAW process |
|---|---|---|---|---|---|
| **GMAW** | 210-240 | 350 | 0.4-0.8 | $ | 0.6 |
| **T-GMAW** | 210-240 | 320 | 0.7-1.6 | $$ | 0.6 |
| **DC-LSND** | 235-245 | 350 | 0.25-1.4 | $$ | 0.6 |
| **K-TIG** | 230 | | 0.3-0.75 | $$ | 0.3 |
| **DE-GMAW** | | 350-550 | 0.3-1.27 | $$$ | 0.2-0.3 |
| **LBW** | 400-420 | | 1-2.5 | $$$$ | 0.1 |
| **HL-GMAW** | 257-270 | | 0.7-2.5 | $$$$ | 0.2-0.3 |
| **SAW** | 215-226 | 450 | 0.4-1.1 | $$$ | 1 |
| **FSW** | 290-350 | 355 | 0.1-0.5 | $$$ | 0.6-1.1 |
| **DSAW** | 200-220 | | 0.1-0.35 | $$$ | 0.2-1.2 |

### *4.2 Automation and robotic programming*

Robotic welding automation allows manufacturers to increase quality, flexibility with the ultimate aim of reducing costs. Many advanced welding processes also rely almost exclusively on robotic manipulation to provide the required control and posture. However, the challenges involved in programming welding robots for either complex environments or low volume production runs have been a significant barrier to shipbuilding. New advancements in the way robots can be automatically programmed are being used to generate robot programs directly from Computer Aided Design models with minimum human input. This now makes it possible for robot welding to be more cost effective than manual welding, even for once-off tasks.

*Automated Offline Programming (AOLP)* Larkin et. al. (2018) is an approach which extends Offline Programming (OLP) by using algorithms to automate much of the robot programming process. This can drastically reduce or even eliminate the human effort required for robot programming and allows for the generation of complex motions to access challenging areas, as well as integrating sensing to deal with part placement inaccuracies. Several shipyards have implemented AOLP with some level of automatic program generation. Kranendonk commercially offer RinasWeld$^{TM}$ as a weld planner, where robot type, position, configuration of external axis, and tooling are all 'hard coded' into a specific version of the software supplied for the end user. Bickendorf (2014) also describes a motion planner termed MOSES for the robotic welding of ship-subassemblies. The general approach taken for each of these AOLP software solutions is shown in Figure 9.

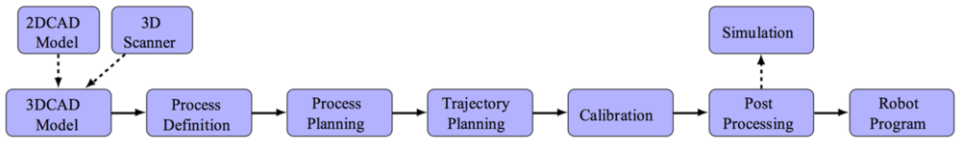


Figure 9: AOLP process for welding. From Larkin et al. (2018).

Unlike Computer Aided Manufacture with conventional multi-axis CNC tools, common industrial robots have a joint configuration which creates redundant motions. When coupled with requirement to provide specific weld gun orientations and other external axes, testing all possible solutions becomes computationally inefficient. By decomposing the welding task space problem, Larkin et. al. (2018) significantly reduce the computational complexity required and significantly simplify the tool path planning problem. This allows for dynamic programming to be handled for changing environments (calibration) and for higher degree of freedom manipulators such as multi-legged crawling robots used for bulk head and ballast tank inspection (Short et. al., 2017). Ding et, al. (2016) use this approach to apply adaptive robotic programming for the wire arc additive manufacture (WAAM) of ship's components. In these instances, AOLP is simultaneously used with CAD part slicing and decomposition algorithms to rapidly generate layered robot welding motion paths.

### *4.3 Additive Manufacturing*

Additive Manufacturing or 3D-Printing (AM) is a technology that produces three-dimensional parts layer-by-layer, generally from polymeric or metallic materials. The method relies on a CAD protocol created digitally and transmitted to a machine that builds the component. Additive Manufacturing offers several advantages in the production of complicated and intricate parts, presenting design freedom with the ability to manufacture single or multiple components from a wide range of materials. The process allows the fabrication of parts from materials, such as refractory metals, titanium alloys, Ni- and Co-based super-alloys, tool steels, stainless steels as well as aluminum alloys, in near-net shape, requiring minimal post-processing. While the process has significant advantages over metal casting, wrought processing or powder-met techniques that require further post-processing (heat treatment and subtractive steps), AM provides easy manufacturing of engineering components that can be used by any industry, including shipbuilding.

For Ingalls Shipbuilding (Ingalls), the Integrated Project Team (IPT) has assessed and demonstrated the use of AM during ship construction activities, quantify the expected benefits, and provide a recommended path toward implementation. For General Dynamics Electric Boat (EB), the IPT has developed and demonstrated a process map that will allow the rapid production of tools and fixtures using AM. Additive Manufacturing (AM) is rapidly becoming a versatile tool in the manufacturing industry as the cost of acquiring and implementing the technology decreases. The Navy Metalworking Center (NMC) has conducted a project that has demonstrated the cost and time benefits of AM to support the construction of Navy platforms. Ingalls and EB are interested in using AM for several potential applications, such as visual aids for manufacturing, planning and staging; and production aids for temporary construction and templates. Using AM for these applications will lead to cost and time benefits, as well as improvements to first-time quality during ship construction (Wang X and Whitworth J, 2016).

On-site testing at Ingalls of three-dimensional (3-D) printed parts has been used to develop an implementation plan and to support a business case. At EB, the project-validated process map has been used as the basis for a procedure to instruct shipyard personnel on how to rapidly deploy new tooling / fixtures using AM. Ingalls has estimated a minimum acquisition cost savings of US$800,000 per year by utilizing AM for the construction of DDG, LHA and LPD. EB has estimated a minimum acquisition cost savings of US$200,000 per Virginia class

submarine (VCS) by using AM technology to rapidly deploy new tooling and fixtures. Implementation at Ingalls is planned in FY17 for DDG 121, LHA, and all future surface combatants produced there. Implementation at EB is planned for FY 17 on VCS (SSN 794) (Ingalls, 2017).

Engineers at Netherlands' Port of Rotterdam have begun experimenting with 3D printing processes to carry out repairs on damaged ships. The Port has opened the Rotterdam Additive Manufacturing Lab (RAMLAB), which has a pair of 6-axis robotic arms capable of additively manufacturing large metal industrial parts. The port is working alongside Autodesk which presented a scaled down 3D printed ship's propeller at Hannover Messe in Germany (World Industrial Reporter, 2017).

Some of the specialized component examples that have been produced via AM include brackets for aircrafts, micro-turbines, medical devices, fuel nozzles for jet engines, vacuum calibration sleeve, wing profile, turbine rotor, hydraulic crossing, etc. The AM industry products and services worldwide are projected at over $11 billion.

Herzog D, et al. (2016) has discussed the methods and materials for AM. In this context, the overview article describes the complex relationship between AM processes, microstructure and resulting properties for metals. It explains the fundamentals of Laser Beam Melting, Electron Beam Melting and Laser Metal Deposition, and introduces the commercially available materials for the different processes. Special attention is paid to AM specific grain structures, resulting from the complex thermal cycle and high cooling rates. The properties evolving as a consequence of the microstructure are elaborated under static and dynamic loading.

### *4.4 Fabrication and joining of composites*

Manufacturing imperfections, like air inclusions, de-cohesions and fiber misalignment, and chemical features, i.e. the influence of ambient and laminate temperature while curing and humidity, may seriously affect the composite strength as well as its failure modes. This aspect is widely covered in literature, and confirmed in recent works by Godani et al. (2014), Kim et al. (2014), and Kalantari and Dong (2017), in addition to earlier references.

#### *4.4.1 Air inclusions*

The presence of air bubbles of various size is common in hand lay-up manufacturing method. The spherical shape of the bubbles make them less critical than sharp de-cohesions originating from impregnability issues, in terms of stress concentration, although they can influence the inter-laminar shear strength up to 25 % as investigated by Di Landro et al. (2017). Shipyards are gradually abandoning the manual impregnation, which is still very common indeed, in favor of the impregnation machines.

#### *4.4.2 Exothermic peak*

The exothermic peak often results in the need of splitting the lamination of thick stacking sequences into multiple stages. The peak mainly depends on the resin curing process, which is a fixed parameter once the matrix is chosen. Relevant investigations include Vargas et al. (2015) for polyester and Park et al. (2015) for epoxy. Other governing parameters are the ambient temperature which can seldom be controlled in shipyards, especially when laminating outdoor, and mostly the laminate thickness, since the heat transfer rate is less efficient in thicker laminates. Infusion method requires expensive consumables that have to be disposed after the process, thus splitting the lamination into different stages significantly increases the manufacturing cost. Moreover, the cured surfaces will not bond over fresh resin by chemical adhesion when produced by infusion, and only mechanical adhesion onto wrought surfaces will be possible. Hence, the vacuum infusion is still limited to decks, super-structures and components for naval applications. In leisure boat industry instead, the thickness involved is

usually not critical in term of exothermic peak, even in the bottom shell, and the manufacturing method choice is governed by a cost-benefit analysis.

#### *4.4.3 Bending response of infusion made composites*

Infusion-made composites present better quality towards embedded imperfection such as decohesions, air inclusions and delaminations. If on one side the higher fiber content associated to the infusion method leads to higher specific mechanical properties, the lower thickness diminishes the inertial contribution on the other. Hence, the resulting laminate will show a reduced bending response. Such assumption has recently found experimental evidence in Yaacob et al. (2017), where a small 12 feet fishing boat was built by both hand lay-up and infusion, with identical stacking sequence. The experiments showed that the resin infusion technique performed better upon ultimate tensile strength (+27%) but less satisfactory for in compressive stress (-12%) and flexural stress (-34%). The thickness reduction also gives rise to concerns about elastic stability issues. In conclusion, the potential benefits led by infusion method are out of discussion and well assessed in terms of composite quality.

#### *4.4.4 Prepregs*

Prepregs represent the state of the art in terms of composite performance, as they can maximize the fiber content leading to outstanding material properties. The extremely high cost and the need for refrigerated storage rooms limit their application to racing yachts and high-performance components. Manufacturing cost of prepreg is also a critical aspect, as to achieve outstanding material performances vacuum bag technology in controlled environment shall be adopted. Godani et al. (2015) highlighted poor inter-laminar performances of prepregs specimens due to air inclusions, with respect to a similar fiberglass composite produced by infusion. Gangloff et al. (2017) showed that imperfections related to air inclusion mainly originate in prepreg production, while the curing process inside the vacuum bag has a scarce influence on the overall quality.

#### *4.4.5 Fibre-matrix interface*

The interface between fibre and matrix is a governing parameter when dealing with fatigue and fracture, as well as dynamic loading. Due to chemical issues related to the different ionicity of matrix and fiberglass, a sizing is always necessary to improve fiber impregnability and fiber-matrix bonding. Carbon fiber is less critical and does not require sizing application in general, although recent innovations made available sizing for carbon, to improve the laminate performance (Andideh and Esfandeh, 2017) and Kobayashi et al. (2017). The fiber-matrix cohesive parameters may determine the predominant damage mode in particular stress conditions, as recently investigated by Ma and Liu (2016). Fiber bridging effects in fatigue problems were investigated by Olave at al. (2015), while Airoldi et al. (2015) showed the influence of fiber bridging in delamination problems

#### *4.4.6 Epoxy matrix*

Vinyl-ester matrices are nowadays characterized by outstanding performances in terms of elongation at break (above 4.5 %), as well as inter-laminar adhesion. These features close the gap with epoxy resin, considered the top performing matrix. Besides the higher cost of epoxy, correct handling of an epoxy matrix is a challenging task, as epoxy requires fixed thermal profiles in the post-curing stage, in order to show clear advantages with respect to a vinyl-ester matrix. Hüther and Brøndsted (2017) found that fatigue performance of unidirectional glass fiber reinforced epoxy composites, for loading at 0° with respect to fiber orientation, is highly influenced by the curing cycle. Relatively small components can be built in pressurized ovens, while large hulls require mold heating: in conclusion, the handling difficulties are still limiting the widespread use of epoxy for large marine structures mainly to racing yachts and naval applications.

### *4.4.7 Non-crimp fibers*

Non-crimp fabrics maintain the planarity of the reinforcement leading to an increment of the tensile strength of about 20 to 30 %, being equal the glass content with respect to a woven fabric, according to an investigation conducted by the author upon reinforcements currently available on the market. Moreover, the lower number of interstitial space between non-crimp fibers also allows an increment in the composite fiber content, leading to a further improvement in terms of mechanical properties. On the other hand, non-crimp fibers are more expensive than traditional woven roving, thus their application is limited to high performance composites. Critical aspects were highlighted by Shiino et al. (2017) in delamination problems, which found a decrease in the surface propagation energy because the stitch yarn replaced the carbon fiber/epoxy interface, which has better chemical affinities.

### *4.4.8 Joining of composites*

Fabrication of the hull either metal or composite is by no means the end of production; the bare hull must be turned into the finished vessel through the addition of stiffeners, decks, superstructure, bulkheads and fittings, all of which must be joined together. This may require up to 50% of the total time and building costs. Joining of fiber reinforced plastic can be achieved by surface bonding, bolted connection or combined solution. When large composite components are considered, bolting is not usually cost-effective since, as the number of bolts increases, the manufacturing process of the joint becomes slow and costly. Also, the bolts are adding weight to composite components. Bonding is cheaper, lighter, needs significantly less assembly time, can join dissimilar materials and FRP, does not change the base material properties, allows the use of thinner plating, can be performed from one side of the panel, and spreads the load over a greater area. Flexible adhesives can also reduce vibrations, compensate for tolerance problems in large component assembly, accommodate thermal expansion differences and reduce stresses due to deformations. Importantly in a marine context, bonding may also replace over-laminating to fix stiffeners to panels, significantly reducing the labour and time required.

Sutherland et al. (2017) conducted a large test program of statistical experimental design techniques, used to study the strength of 'T'-Joints representative of various connections of marine composite. The effects of different surface preparations, cleaning methods and adhesives were investigated. An analysis of variance was conducted, giving an extremely good fit to the experimental data while statistical methods identified significant interaction effects. A way to overcome these problems is to prefabricate metallic joint elements (special profiles), which are adhesively bonded to the composite substructure by the FRP manufacturer and then welded to the ship structure. Such a procedure allows the adhesive joint to be manufactured in a suitable environment and, on the other hand, the shipyard to weld the FRP parts to the ship in an equivalent manner as corresponding metal parts. The majority of research carried out on metal-to-composite connections has been on secondary process joints. Some assessment strategies for composite-metal joining technologies is reviewed by Jahna et al. (2016). This involves the manufacturing of a composite structure and subsequent adhesive bonding to the metallic structure. There is increasing interest in producing joints by the co-curing method, which involves the making of the joint while consolidating the composite material.

### *4.4.9 Influence of the ply orientation*

Hazimeh et al. (2016) was investigated the influence of composite laminates' orientation on the peel and shear stresses in the adhesive layer of composite double lap joints. The highest adhesive stresses are achieved when fibers are all or mostly oriented along the loading/axial direction [0°] and the lowest adhesive stresses are obtained when the fibers are oriented perpendicular to the applied load [90°]. It is concluded that the adhesive stresses increase as the substrates longitudinal stiffness increases. Stress in the adhesive layer is mostly influenced by the closest laminate plies and almost not affected by the far plies.

#### *4.4.10 Nanoparticles*

Findings from nanoscience and nanotechnology, influence adhesives sciences significantly. Akpinar et al. (2017) added nanoparticles to the adhesive to increase the damage load of adhesively bonded single lap composite joints. Tensile and bending moment damage loads were experimentally investigated. In his study, carbon fiber fabric reinforced composites (0/90°) with Plain Weave were used as the adherend; rigid, tough and flexible adhesive types were used as the adhesive and 1 wt% Graphene-COOH, Carbon Nanotube-COOH and Fullerene C60 were used as the nanoparticles. The use of carbon fiber fabric reinforced composites as the adherend considerably increases the damage load of the joint, depending on the adhesive type. The addition of nanoparticles to the adhesive was also shown to increase the tensile and four-point bending damage load of joint, depending on the adhesive and nanoparticle type.

#### *4.4.11 Fire resistance*

According to the IMO (2009), composites must be considered combustible materials resulting in critical safety issues. Relevant published works include Evegren at al. (2014), Evegren and Hertzberg (2017). Current researches focus on flame-retardant additives: hybrids of aluminum hypophosphite and ammonium polyphosphate proved to be very effective by Lin et al. (2016), as well as phosphorus-containing star-shaped flame retardant included in the polyester matrix as tested by Bai et al. (2014), by the way their impact on mechanical properties was not assessed. Saat et al. (2017) tested the influence on mechanical properties of aluminum phosphate, used as fire retardant in fiberglass reinforced polyester matrix for leisure boat applications, indicating promising results.

## 5. QUALIFICATION AND APPROVAL

Technology qualification is all about building confidence for the stakeholders. New materials (e.g. composites) and related fabrication processes offer several benefits like weight saving, integrated functions etc. which finally result in reduced life cycle cost of ships and marine structures. They also offer a large variety of materials, fabrication and assembly processes which will in future lead to a much larger material mix in ships and offshore structures.

On the other hand, marine structures need to survive under extreme environments and operational conditions (loads, exposure to sea water, chemicals, UV radiation) for long life spans with limited possibilities of human interaction at sea. This imposes high risks on human life, maritime assets and the marine environment. To manage those risks rules and regulations by IMO, SOLAS (supervised by the flag states) as well as the classification societies have been issued, against which any new material and fabrication process needs to be benchmarked and approved.

In relation to the approval of new materials and related fabrication processes currently the maritime industry is facing the following challenges:

- New materials offer a wide variety of options which all influence their properties. Long term experiences on their operational performance are often missing;
- Prescriptive rules and regulations are often not applicable to new materials. Therefore, equivalent safety needs to be demonstrated for alternative designs, arrangements and innovative solutions. While this process as such is well known, its implementation is case specific and currently not harmonized, knowledge intensive, lengthy and costly;
- The speed of innovation in the maritime industry as well as in its suppliers (e.g. material sciences) is increasing and becomes a competitive factor. Current approval practices become more and more obstacles for innovation or slow down the innovation process significantly. A new – faster and simplified - procedure to approve new materials is necessary.

Putting into practice new materials or technology will need to be proven and qualified prior to be set in production and operation to minimize risk for its developers, manufacturers, vendors, operators and end-users. New goal based design codes give more options for material and process selection.

This chapter is divided into two main parts; one presenting the outcome from an ISSC meeting with the industry and example of qualification of composites for the offshore industry and the second part show the different class society approval and qualification schemes.

### *5.1 Qualification of composites*

Lack of rules and guidelines can be a showstopper for implementing new material solutions. For the maritime sector, guidance related to use of composites has been limited. However, the issuing of the IMO guidelines for use of fiber reinforced plastic (FRP) within ship structures were formally approved without objections at MSC 98 the 16 June 2017 are welcome guidance for designers. The guidelines will be "interim" for a period of four years to allow for feed-back and modifications based on experiences from applying the guidelines. The guidelines particularly address fire when FRP composite is used to replace non-combustible structures. The document provides guidance when developing lightweight ships of the future with focus on recommendation regarding the needed assessment to prove equivalency by compliance with the prescriptive requirements provided by SOLAS with focus on risk assessment and uncertainty treatment. Still there will be challenges the industry will face and in order to map and discuss these, a joint workshop facilitated by this ISSC committee were held in April 2017, see below for a summary.

#### *5.1.1 Hamburg meeting on qualification on composites*

With the aim to discuss obstacles and possible new approaches for the approval of new materials in the shipbuilding and offshore sectors a joint workshop was arranged between the ISSC “Fabrication” committee, the European research projects RAMSSES and FIBRESHIP, see Chapter 2.1.2, and other participants including the classification societies DNVGL, Bureau Veritas and Lloyds Register and a representative of the IMO Correspondence Group on Composite Materials. The participants presented different approaches to improve the approval process for new materials which are either in use by the classification societies or under development in research projects. In addition, the group consisting of some 15 participants developed a list of issues to be addressed. This topic list was discussed and prioritized after the workshop. The discussion will continue using the E-LASS platform (www.e-lass.eu) which is open to external participants at no cost.

The following list gives an overview on the outcomes of the joint workshop conducted in Hamburg in April 2017:

- Spreading knowledge and establishing a “Maritime Materials Innovation Platform”
  - Establish a platform for information exchange and discussion;
  - Demonstrate and showcase successful applications of composite materials in the maritime sector;
  - Provide a better overview on existing rules and regulations related to new materials in shipbuilding and offshore, harmonize rules and approaches for shipbuilding and offshore;
  - Improve information exchange with other sectors and cross-industry standardization;
  - Develop materials, component and test data bases and define access rules for joint use.

  Note: The European RAMSSES project together with the existing E-LASS network for maritime lightweight materials are in a process to establish and extend such a platform which is accessible to any interested party, see www.e-lass.eu

- Research and research infrastructure
  - Research to better understand failure mechanisms of new materials and components under maritime conditions, with focus on ageing;
  - Assess defects in mock-ups from previous research and application;
  - Improve and share infrastructure for long term testing under real-life conditions;
  - Better correlate long-term testing, accelerated lab tests and develop numerical methods to reduce expensive tests;
- Supporting the prove of equivalent safety per SOLAS:
  - Collect success stories for the use of composite materials and submit to IMO;
  - Develop standard risk scenarios, which can be re-used for similar cases to reduce the effort and time for risk assessments;
  - Develop and harmonize rules on required tests depending on risks across classification societies and sectors;
  - Define "experience classes" and a concept to implement them in the approval process;
  - Define procedures how condition monitoring in operation can be considered in the approval process;
  - Develop a list of "qualified service suppliers" for inspection, NDT, repair and eventually recycling of composite and hybrid material solutions;
  - Develop lists of approved NDT methods and numerical methods for design;
  - Extend the list of type approved solutions for materials, components and processes.
- Develop new prescriptive rules for low risk composite applications with sufficient experience;
- Develop new business models for risk sharing in the introduction of innovative solutions between

### *5.1.2 Best practice of qualification of composites*

Composites is an attractive material due to its strength, light weight and enhanced resistance to $CO_2$ and $H_2S$. Certification and qualification of composite components qualification requires extensive testing including full scale testing to document especially long-term properties.

A typical qualification campaign for a subsea composite component is costly and can range from 10 to 100 MNOK and an approximately cost distribution is shown in Figure 10 and reply on physical testing and very limited analytical work.

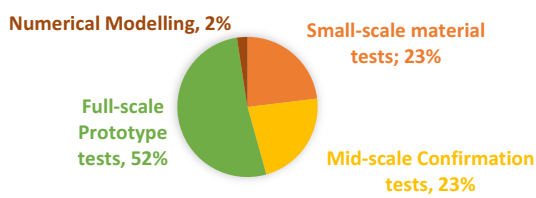


Figure 10: Approximate cost distribution for a typical qualification program for use in an oil & gas application

Since a test campaign is both costly and time consuming, qualification by simulation to reduce the need for testing would be of high value for both offshore and the maritime industry. Today industry phase the challenge to develop and qualify advanced material models to predict long-term performance of composites structures. Multi-scale modelling is important and should address important factors like the effect of aging of material at various medial, temperature and failure mechanisms to be assed under both short term and long term loading conditions (cyclic and static fatigue). DNVGL-ST-C501 "Composite Components", 2017 is a generic composite standards which give guidance on required test scope and acceptance criteria. The standard

opens for several ways of documenting the material properties like; direct measurements, qualification against representative data, qualification against manufacturer's data, data from the open literature and by component testing. The standard is adopting a multiscale approach where the results from smaller scales can be reused for various applications with different load scenarios, see Figure 11 for a possible test scheme.

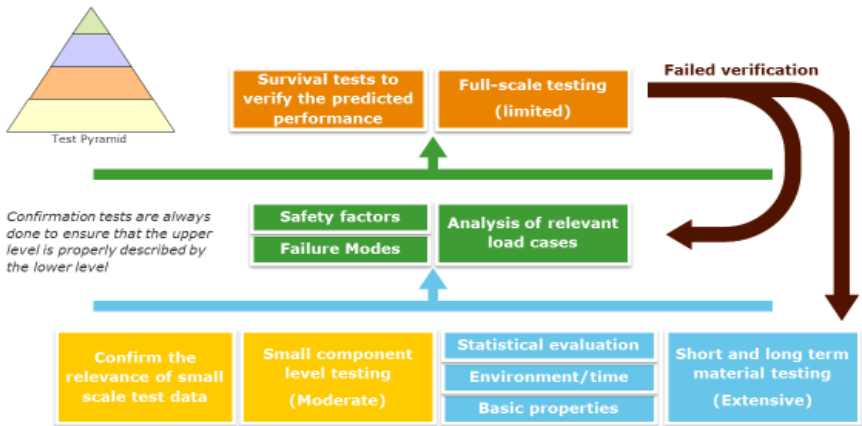


Figure 11: Overview of a proposed test campaign for composite material

Below some different theories and modelling assumptions have been pretended.
Performance based qualification approach can be useful for application where a well-known simple performance is required;

- Many full-scale tests are typically required depending of the targeted performance accounting for environmental effects such as temperature and degradation.
- The qualification is only valid for the tested conditions.
- Not a practical option when a complex long term performance is required.

Short and Long Term Small-scale Material Testing is demanding and may become expensive;

- Flexible with statistically determined characteristic values are used.
- Long term material strength is determined by small-scale testing.
- All determined properties are used in the analysis phase.
- Results of material tests depending on their scatter are used to choose the right set of calibrated partial safety factors.

Confirmation Testing on Representative Component;

- To ensure the relevance of material tests to the actual component.
- Static tests: Stresses/strains to failure should be within one standard deviation of the predicted mean stresses/strains.
- Long-term tests: Time/cycles to failure should be within one standard deviation of the predicted mean Time/cycles.
- Can be used for determination of the model factor accounting for the deviations between tests and analysis predictions.

Survival tests are required to verify the long-term strength calculations;

- Required only for safety classes high and medium.
- Should be performed for the loads which FRPs are expected to experience.
- Two survival tests for safety class high for each load case.
- One survival tests for safety class medium for each load case.

There has been activity the last years to qualify composites pipes for use subsea like a spolable reinforced thermoplastic pipes (RTP) as a cost-effective solution compared to carbon steel or CRA material (Adam et al., 2016). Anderson et al. (2016) investigated the use of flexible composites risers for 3000 m water depths where weight and installation cost can be reduced by use of composite pressure armour/tensile armours to replace steel. Wilkins et al. (2016) presented a qualification program for composite pipes based on a risk based approach (DNVGL-RP-A203 Technology Qualification 2017) in combination with generic composites requirements given in DNVGL-ST-C501. The test campaign consisted of small, medium and large scale testing. The paper addresses the challenging related to different acceptable small scale test methods to measure strength of composites materials, depending on method mean strength of 400 MPa up to 1000 MPa were reported. The data from small scale tests were input to finite element models of the pipe, and the medium scale testing was validating and adjusting the numerical models to capture the damage and failure mechanisms. To appropriate address the failure criteria is challenging when modelling composites; from assuming simple linear material behavior up to the point of brittle failure "fiber strain models" to progressive damage models allowing for matrix cracking.

### *5.2 Qualification and approval processes by the class societies*

Technology qualification is a process of defining an adequate set of acceptance criteria for delivery and limits to operations, to assure defined technical performance of solutions. In the following the qualification and approval schemes by the different class society is briefly presented and discussed.

#### *5.2.1 DNV GL*

Technology Qualification comprises services for qualifying, assessing and developing new technology, as well as failure investigation. These services typically involve laboratories and physical testing. DNV GL has two recommended practices which addresses new technology; Technology Qualification / DNVGL-RP-A203, 2017 / and Technology Qualification Management / DNVGL-SE-0160, 2015 /DNV-DSS-401, 2012/. These practices have successfully been used by the offshore and the maritime industries. To focus on where uncertainty is greatest, the novelty categorization of Table 5 can be used. Both the novelty of the technology itself and its application area affect the uncertainty associated with the technology.

Table 5: Technology Categorization

| Technology Categorization (table 7-1 in DNV-RP-A203) | | | |
|---|---|---|---|
| Application Area | Degree of novelty of technology | | |
| | Proven | Limited Field History | New or Unproven |
| Known | 1 | 2 | 3 |
| Limited Knowledge | 2 | 3 | 4 |
| New | 3 | 4 | 4 |

Category 1 technology elements are proven with no new technical uncertainties, where proven methods for verification, tests, calculations and analysis can be used to provide the required qualification evidence. Elements in category 2 to 4 require technology qualification and have an increasing degree of technical uncertainty.

#### *5.2.2 ABS*

ABS has two documents that deals with new technology; Qualifying new technologies and Guidance Notes on Review and Approval of Novel concepts (April 2017). The guidance is based on an engineering approach for qualification and is divided into a multi-stage process that is aligned with the typical product development phases of a new technology. For the

validation system integration and operational stage typically engineering evaluations and risk assessments are carried out. For both certification and classification approval concepts the acceptance will be based on safety and includes vendor, system integrator and end-user. The process covers the following qualification steps; feasibility, concept verification and prototype.

#### *5.2.3 Bureau Veritas*

The qualification of new technologies or existing technologies used in a new context is described in Bureau Veritas guidance note NI525 from 2010. The basic principle of qualification is to simulate, as realistically as possible, the service conditions for which a novel technology is designed. The qualification process opens for combining both theoretical, analytical modelling and physical tests. The process is divided into five steps; (1) identification of new technology, (2) functional description, (3) failure mode effect and criticality analysis (FMECA), (4) cost/benefit analysis and (5) recommendations regarding design, qualification and inspection/maintenance of equipment as to reduce/maintain the deviation from specified performances and/or risk to/under an acceptable level.

#### *5.2.4 Lloyds*

The qualification process is divided into three steps; technology appraisal, technology qualification (TQ) plan and execution, review and certification and described in Guidance Notes for Technology Qualification from 2017. The TQ is a goal based approach to risk that can be applied to any technology, ranging from the unconventional LNG offloading arrangements to the integration of marinised gas turbines into topside process plants, as well as aerial vehicles and various renewable technologies.

#### *5.2.5 IMO*

The IMO guidelines for how to manage fire safety in association with use of fibre reinforced plastic (FRP) within ship structures (MSC.1/Circ.1574 ) were formally approved without objections at MSC 98 in 16 June 2017. The guidelines will be "interim" for a period of four years to allow for feed-back and modifications based on experiences from applying the guidelines. This is hence a challenge to the industry to demonstrate interest in lightweight structures and to apply and evaluate the guidelines. The guidelines particularly address necessary fire safety considerations when FRP composite is used to replace non-combustible structures. The document provides guidance when developing lightweight ship structures, with focus on recommendations for the required assessment to prove fire safety equivalency to compliance with the prescriptive requirements. This approval process for alternative design and arrangements is provided by SOLAS II-2/17 (fire safety) and by SOLAS I/5 (general) and is based on risk assessment evaluation of introduced hazards and achievement of fire safety functions. The guidelines for example describe typical FRP composite materials and compositions used in shipbuilding with regards to fire behavior and give recommendations for relevant fire testing and for the fire risk assessment methodology. Furthermore, potential deviations against prescriptive fire safety regulations are described and issues other than related to fire safety are exemplified. The guidelines are intended for the approving Administrations when reviewing alternative designs involving FRP composite, but the guidelines will not less be used to support ship design and preliminary evaluations.

## *6.* BENCHMARKS AND CASE STUDIES

### *6.1 Uncertainness in welding simulation*

In numerical welding simulations, each selected parameter such as mesh size, material modelling, heat input, boundary conditions play an important role. In order to understand the influence of the modeler's practice and FEM codes on the welding simulation, the benchmark study was initiated in the ISSC 2015 V.3 Committee. Only the preliminary results were reported

in the previous committee's and thus, a short summary is included into the ISSC 2018 report. The details of the study is published in Caprace et al. (2017).

The geometry considered was a T-joint typically used for stiffened panels in ships and offshore structures. A 12-mm-thick stiffener was welded to the base plate that has a length of 500 mm. Both base plate and stiffener were the low carbon grade DH36 ferric steel plate. The welding residual stress and distortion were analyzed numerically, and the results were compared to the experiments. In welding experiments, (FCAW) single-side one pass welding procedure with a heat flux of 10.7 kJ/cm were applied. All the benchmark participants received the same technical specification about welding experiments. The responsibility to interpret this document, considering the limitation of each software, relied on the modelers. Thus, the variability of the solutions (S1-S6) adopted by the experts to solve the same problem; see Table 6. There are the combination of 4 different software, 3 thermal boundary conditions, 3 mechanical boundary conditions, 2 similar material models, 4 equivalent heat sources and 4 meshing. As seen from Table 7 an average element size was about one millimeter for all cases. To simulate the material deposition during the welding process, the element birth & death technique was employed.

Table 6: Simulation matrix. From Caprace et al. (2017).

| Sim Id | Software | Therm. BC | Mec. BC | Material Prop. | Hardening Model | Phase Transf. | EHS Model | Elem. Type |
|---|---|---|---|---|---|---|---|---|
| S1 | Ansys | conv.+rad. | MBC1 | $M_1$ | Isotropic | No | USHF | 8N-Parallelepiped |
| S2 | Ansys | conv.+rad. | MBC1 | $M_1$ | Kinematic | No | USHF | 8N-Parallelepiped |
| S3 | Sysweld | conv.+rad. | MBC1 | $M_1$ | Isotropic | Yes | Goldak's | 8N-Parallelepiped |
| S4 | Sysweld | conv.+rad. | MBC1 | $M_1$ | Isotropic | No | Goldak's | 8N-Parallelepiped |
| S5 | Virfac | conv. | MBC3 | $M_1$ | Isotropic | No | Goldak's | 4N-Tetrahedral |
| S6 | Abaqus | conv.+rad. | MBC2 | $M_2$ | Isotropic | No | Goldak's | 8N-Parallelepiped |

Table 7: Meshing parameters for finite element models. From Caprace et al. (2017).

| Sim Id | Elem. Type | Therm. Elem. Order | Mech. Elem. Order | Node Nbr | Elem. Nbr | $l$•$w$•$hmm$•$mm$•$mm$ | Elem Kill & Alive |
|---|---|---|---|---|---|---|---|
| S1 | 8N-Parallelepiped | 1st | 1st | 33337 | 28392 | 9.60•1.00•0.75 | Yes |
| S2 | 8N-Parallelepiped | 1st | 1st | 33337 | 28392 | 9.60•1.00•0.75 | Yes |
| S3 | 8N-Parallelepiped | 1st | 1st | 194568 | 171600 | 9.60•1.00•0.75 | Yes |
| S4 | 8N-Parallelepiped | 1st | 1st | 194568 | 171600 | 9.60•1.00•0.75 | Yes |
| S5 | 4N-Tetrahedral | 1st | 1st | 127155 | 103302 | 0.78•0.78•0.78 | Yes |
| S6 | 8N-Parallelepiped | 1st | 1st | 82614 | 70760 | 2.25•2.25•1.0 | Yes |

Figure 12 shows the results for the temperature comparison. A good agreement for the maximum temperatures between the experimental measurements and numerical simulations although S6 presents a moderate overestimation. The reason for this might be the difference of thermal boundary condition (heat transfer coefficient) and thermo- mechanical properties (conductivity at high temperature). The cooling rate is also a good agreement with the experiments for the majority of the simulations. The simulations S3 and S4 with uniform surface heat flux (USHF) presents a higher cooling rate than that of the experiments. The simulation S6 maintain the gap observed in the peak temperature almost constant during the cooling. The comparison of fusion zone showed some discrepancies in penetrations, but the size of fusion zone was similar for the simulations and experiments. The results indicates that the change of heat source type and parameters affects peak temperatures and the fusion shape. Furthermore, it seems that the surface convection and radiation (S5) had little effect on the fusion zone shape.

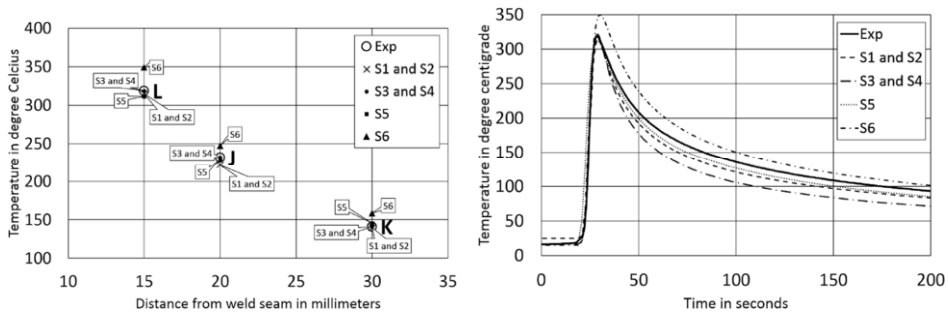


Figure 12: Comparison of the maximum temperatures (left) and Cooling rate for first weld at the point L (right). From Caprace et al. (2017).

The comparison of the welding angular distortions did not revels significant differences, less than 12%, that modeller practices had a small influence on the simulated welding distortion. Simulated residual stress showed higher difference. The measured and simulated residual stress are shown in Figure 13. The highest tensile longitudinal residual stresses were observed in the fusion zone and heat-affected zone as expected. The transverse residual stress induced in the weld and plate is much smaller than the longitudinal residual stress. The distribution of the longitudinal stress is not symmetrical due to the effects of the welding sequence. The longitudinal residual stresses present a good predictability, i.e. less than ≈18% difference. The transversal residual stresses are largely underestimated, i.e. difference largely higher than 35%. This discrepancies can partly due to the imperfect material model. This highlights the need of extensive material testing for welding simulations. The benchmark study show also that the results obtained with the double ellipsoidal heat course model (S3-S6; Goldak's) are closer to the experiments than that of USHF (S1-S2). The insignificant differences between the results S1 and S2 indicates that the kinematic hardening model can be replaced by an isotropic hardening model in this peculiar case. In addition, the effect of phase transformation on residual stresses and distortion seems to be insignificant since the difference between models S3 and S4 was small. Therefore, the phase-transformation can neglected for low-carbon steels (Deng, 2009). The differences due to software's and boundary conditions was less sensitive than other parameters.

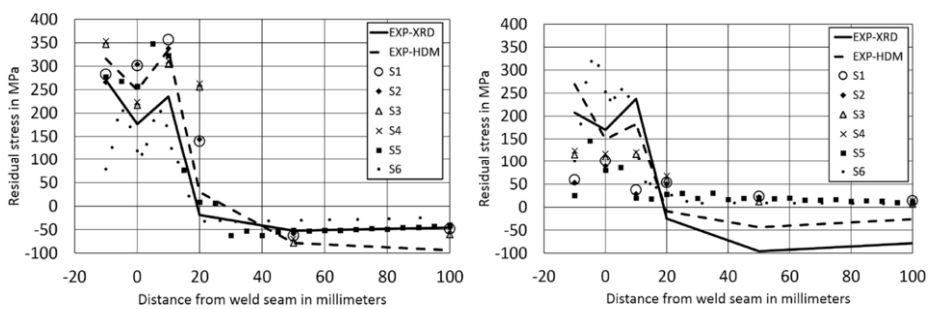


Figure 13: Longitudinal (left) and transversal (right) residual stress comparisons. From Caprace et al. (2017).

### *6.2 Sensitivity analysis on the cohesive parameters of a carbon-steel single lap*

The present investigation aims at assessing the sensitivity of the parameters that define the traction separation law on the de-bonding of a single lap joint. Namely, two finite element software were compared, ADINA and LS-DYNA: the former adopts a bilinear traction separation laws, while in the latter both bilinear and trilinear curves were tested. The results were compared to previous experiments by Tomaso et al. (2014), available in literature.

### *6.2.1 Model Description, material properties and mesh size*

The specimen, which measures 25 mm in width, is described in Figure 14. The resulting cohesive area is 12.5 x 25.0 mm$^2$. The specimen is clamped at both ends with fixes rotations, whereas one end can experience axial translation to apply the tensile force. The composite is made mostly by unidirectional carbon fibres in an epoxy matrix, with a negligible amount of ±45° layers and other non-structural plies to improve impregnation and resin distribution.

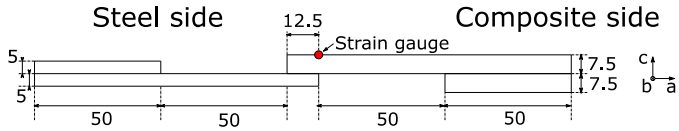


Figure 14: Model description

Steel is modelled as plastic-isotropic, with Young Modulus $E$=203 GPa and $\nu$=0.3 [-]. The yield stress is $\sigma_y$=315 MPa and the ultimate stress $\sigma_u$=455 MPa. The hardening modulus is $E_t$=0,717 GPa.

The carbon reinforced plastic is modelled as elastic orthotropic, the elastic moduli are respectively $E_a$=38.7 GPa, $E_b$=$E_c$=6.5 GPa; the Poisson coefficients are $\nu_{ba}$=0.35, $\nu_{ca}$=0.059, $\nu_{cb}$=0.34.

An eight-node solid element was used in both software due to compatibility issues with the cohesive element. The maximum element edge size was set to 1.07 mm after a preliminary mesh sensitivity analysis, resulting in five layers of elements through the thickness for the steel, and seven for the composite.

### *6.2.2 Cohesive model*

Cohesive elements are modelled in the overlapping area between steel and composite. In ADINA, the element has an initial thickness equal to zero, while LS-DYNA requires a non-null initial thickness, which was set to 0.5 mm. The cohesive element is defined by a traction separation law, which relate the interface traction to the nodal displacement, such law is triangular by default in ADINA, while LS-DYNA allows more complex functions: in the present work both triangular and trapezoidal laws were tested.

In a triangular traction separation law, three parameters define the cohesive separation:

- The penalty stiffness $k$, which defines the steepness of the initial linear part of the law
- The energy release rate $G_{ic}$, which is the signed area under the curve up to the maximum opening displacement, at which separation occurs
- The peak traction $\tau_{max}$, defining the maximum point in the traction-separation law

A trapezoidal law can be defined by the same parameters, although once the peak traction is reached, it remains constant in the so-called plateau region for a certain range of displacements, before dropping to zero.

Once $k$ and $\tau_{max}$, are defined, the parameter $G_c$ also defines the maximum opening displacement.

The cohesive law can be defined separately for mode I and mode II. The cohesive behaviour can act independently for the two modes, or it can consider a mixed mode opening behaviour. In the present work, the power law defined in Equation 1 is considered, and the influence of parameter α investigated.

$$\left(\frac{G_I}{G_{IC}}\right)^{\alpha} + \left(\frac{G_{II}}{G_{IIC}}\right)^{\alpha} < 1 \quad (1)$$

The separation occurs once the inequality 1 is no longer satisfied. $G_i$ is the signed area defined by the separation law at a specific load step.

### *6.2.3 Reference cohesive parameters*

The following reference parameters, derived from literature work and previously adopted by Tomaso et al. (2014) were chosen:

- $G_{Ic}$=140 Jm$^{-2}$; $G_{IIc}$=280 Jm$^{-2}$
- Peak traction, mode I: $\tau_I$=7.6 MPa Peak traction, mode II: $\tau_{II}$=54 MPa
- $K$=5.6·10$^{14}$ Nm$^{-3}$ (Initial opening displacement: $v_c$=0.0000135 mm)
- $\alpha$=0

### *6.2.4 Experimental/numerical comparison and influence of parameter k*

The results, in terms of axial strains, are compared to those achieved by strain gauges placed at different spots in the specimen. For sake of shortness, only the comparison with the strain gauge shown in figure 14 is reported. The penalty stiffness is varied in the range [3.8·10$^{12}$- 5.6·10$^{14}$] for LS-DYNA and [10$^{11}$-10$^{16}$] for ADINA.

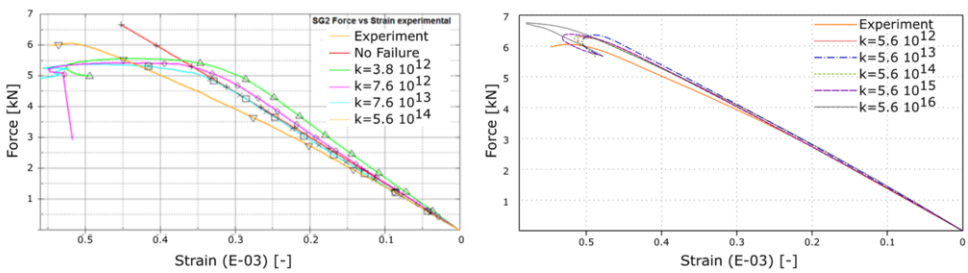


Figure 15: Axial strain for different $k$, LS-DYNA left and ADINA right

From Figure 15, it can be seen how LS-DYNA model is more sensitive towards the penalty stiffness with respect to the ADINA model, by the way the influence of this parameter is quite poor in both cases. ADINA matches the experimental data better, while LS-DYNA underestimates the local axial strains for the strain gage data reported. Data from other strain gauges show opposite behaviour, where LS-DYNA overestimate axial strains, while ADINA still show good experimental matching. In terms of axial force, ADINA generally over-estimate the ultimate force, while LS-DYNA underestimates it.

The failure load, for the models with different penalty stiffness $k$, is also plotted and reported in figure 16. Figure 16 shows a quite constant value of axial force at failure in the range 10$^{11}$-10$^{16}$, though LS-DYNA covers a smaller range. Outside such range the numerical results quickly diverge, in agreement to the behaviour described by Song et al. (2007). In conclusion, it can be said that the penalty stiffness, if chosen in a reasonable wide range, has poor influence on the numerical results, and a rough approximation of such value is sufficient.

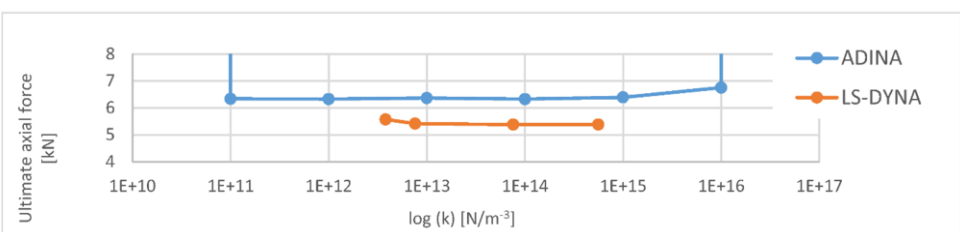


Figure 16: Axial force at failure, function of $k$

### *6.2.5 Influence of $G_c$*

The influence of the parameter $G_c$ on the failure load of the single lap joint is then shown in Figure 17 considering a contemporary variation for both $G_{Ic}$ and $G_{IIc}$, expressed in % value. The bilinear traction-separation law shows a fairly linear trend in the area around the reference value in both ADINA and LS-DYNA, although in ADINA the parameter has a greater impact in the determination of the failure load. The LS-DYNA trilinear law leads to slightly different behaviour, but the impact is minimal in terms of failure force.

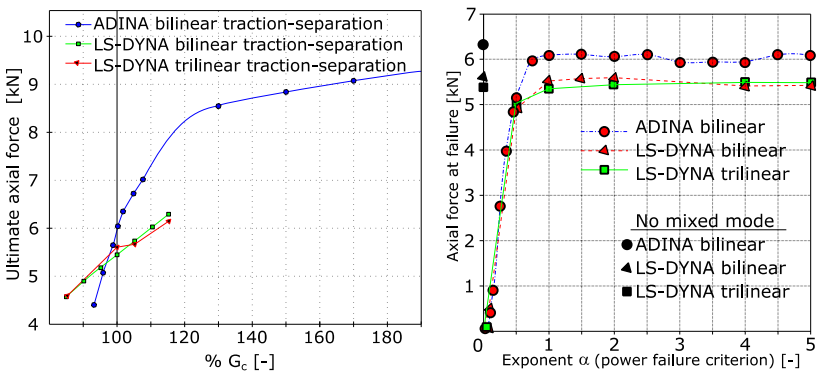


Figure 17: Impact of $G_c$ (left) and $\alpha$ (right)

### *6.2.6 Influence of α*

Finally, the parameter α described in equation 1 is investigated. It is worth nothing that in the present case a predominant mode II opening behaviour is expected, although the bending moment, led by the misalignment of the two parts of the joint, also induces some mode I components. For $0<\alpha<1$, the mixed mode leads to a quick drop in the failure force due to the increment of the contribution of each mode in Equation 1. The parameter has similar impact on both ADINA and LS-DYNA software, with similar decrement for $\alpha<1$.

### *6.3 Fatigue life improvement using HFMI treatment*

This benchmark studies on numerical simulation technique for fatigue life improvement of welded joints by High Frequency Mechanical Impact (HFMI) treatment. Its analyses are conducted as a joint project of Chalmers University of Technology (CUT), Osaka University (OU) and Pusan National University (PNU).

HFMI makes use of cylindrical indenters which are accelerated against a component or structure with high-frequency (> 90 Hz). The introduction of compressive residual stresses (RS), work hardening, and reduce the notch effect at the weld toe are the three main contributions from this HFMI treatment e.g., Marquis (2013). However, there is concern that this compressive RS might deteriorate due to RS relaxation under cyclic loading, and the HFMI treatment might lose its effectiveness. It is needed to develop a numerical simulation technique for compressive RS's development (in welding and HFMI treatment) and relaxation (under cyclic loadings).

Numerical simulations of the HFMI-process have been investigated by many researchers e.g., Foehrenbach et al. (2016), Shengsun et al., (2016), Khurshid et al. (2017). Explicit elastic-plastic finite element (EPFE) code (e.g., Abaqus Explicit) was utilized in order to take into account dynamic effect in those studies. They examined the influence of the FE mesh and various analysis parameters (e.g., friction model, tool indentations, boundary conditions, etc.) on RS distribution, but recommendations on FE meshing and choice of simulation parameters for practical applications to marine structures has not been presented yet.

The objective of this study is set out best practice guides with respect to those simulations. This study is composed of three parts: a) HFMI simulation for stress-free steel sheet; b) welding-HFMI simulation of a welded joint; c) residual stress relaxation under cyclic loadings.

*6.3.1 Multiple impact simulation of the HFMI process on stress-free steel sheets*

The analysis target is HFMI-treated flat sheets of S355J2H (10 mm thickness) studied by Ernould et al. (2017). These sheets were manually treated along a path of 30 mm. A pin with a tip radius of 2 mm and a travel speed of 12 cm/min were used. RS were measured at the groove center by means of X-ray and neutron diffraction up to a depth of 5 mm. RS at the surface were respectively -200 and -400 MPa along the transverse and longitudinal (x-dir.) direction. Maximum compressive residual stress of -550 MPa is obtained at 0.8 mm depth in the transverse direction.

HFMI simulations are either displacement controlled simulations (DCS) or force controlled simulations (FCS). The pin's impact velocity has to be prescribed in FCS, but is difficult as a matter of practice, especially for manually treated cases. Therefore, DCS is chosen in this study. For simplicity, the pin is modelled as a rigid, and it is assumed that the indentation depth and impact period are constant.

Ernould et al. (2017) performed DCS of the target flat sheets, and reported fair agreements in RS profile with the experiments observed with combined isotropic-kinematic hardening law. The effectiveness of the analysis parameters chosen in their report was examined in this study.

The FE mesh shown in Figure 18 is used in the analyses. (x, y, z) coordinates shown in this figure are used in following discussions. This model features the same specification as those of Ernould's model. It is composed of hexahedron brick elements. All nodal displacements are constrained on the bottom face, and the transverse (y-dir.) motion is fixed on the symmetric plane. Peening tools are modeled by rigid shell elements. The peening pin is given an enforced oscillating motion along its axis with a constant frequency, such that the pin impacts the center of the plate. The indentation depth of $D$=0.2 mm is assumed. A linear motion in x-direction with a velocity such that every impacts are spaced by the given pitch $P$ for the given pin frequency $f$. Friction coefficient of $\mu$ = 0.3 between pin and workpiece, and radii of pin nose of $R$ = 2.0 mm are given. Hereafter, this procedure is called 'multiple impact' simulation (MIS).

The Chaboche's combined isotropic-kinematic and strain rate dependent hardening raw is adopted. In this hardening law, back stress tensor is given by the equation below:

$$d\boldsymbol{\alpha} = \sum_{i=1}^{M} d\boldsymbol{\alpha}_i \,;\; d\boldsymbol{\alpha}_i = C_i \frac{dp}{\sigma_o}\left(\boldsymbol{\sigma} - \boldsymbol{\alpha}\right) - \gamma_i \boldsymbol{\alpha}_i dp \tag{2}$$

where, $\boldsymbol{\alpha}$ is back stress tensor, $\boldsymbol{\sigma}$ is the stress tensor, $\boldsymbol{\varepsilon}^p$ plastic strain tensor, $C_i$, $\gamma_i$ are material parameters, $dp$ accumulated equivalent plastic strain increment, $M$ number of kinematic parts, and $i$ part number. $M$ = 2 is used in this study. $\sigma_o$ is the yield stress, and its developing equation is given as:

$$\sigma_o = \sigma_{o,0}\, F(\dot{\varepsilon_{\mathrm{p}}})\, G(\varepsilon_{\mathrm{p}});\;\; F(\dot{\varepsilon_{\mathrm{p}}}) = 1 + \left(\dot{\epsilon_{\mathrm{p}}}/_{H}\right)^{1/\rho}, G(\varepsilon_{\mathrm{p}}) = 1 + a(\varepsilon_{\mathrm{p}})^{b} \tag{3}$$

Here $\sigma_{o,0}$ is the initial yield stress, $H$ and ρ are Cowper-Symonds strain hardening parameters, and $a$ and $b$ are isotropic strain hardening parameters. Material parameters are the same as those adopted in Ernould et al. (2017), and are listed in 'Optimized' column of Table 8.

Young's modulus $E$ = 210 GPa, and Poison's ratio $\nu$ = 0.3. In Equation 2, $\gamma_1 = 2.19 \cdot 10^2$ and $\gamma_2 = 1.07 \cdot 10^2$. For Equation 3, $a = 1.0 \cdot 10^{-6}$ and $b$=0.6. $\rho$ = 5.80 in accordance with Yasuda and Rashed (2016). Peening is carried out on the intersection between the top face and the

symmetric plane over 10 mm. $f$ = 100 Hz is assumed because it was found that the peening response is not depending much on the frequency in the preliminary analysis.

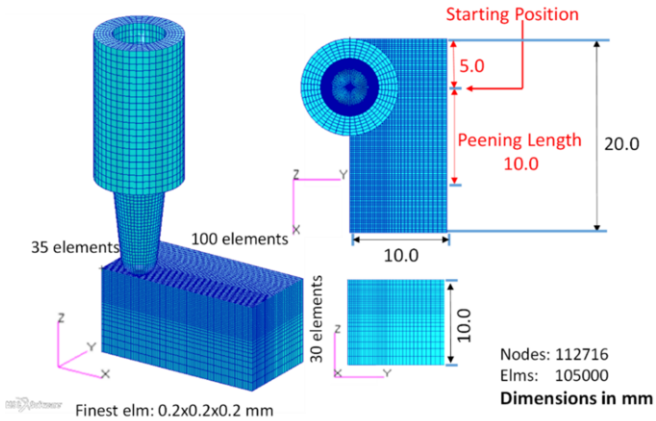


Figure 18: FE mesh of the flat sheet and peening tools used in multiple impact simulations.

OU and PNU performed peening analyses using different explicit EPFE codes (OU: MSC DYTRAN (MSC Software, 2017), PNU: Abaqus Explicit (ABAQUS Inc., 2016)). They searched optimal simulation parameters, and found that simulated RS profile agreed well with that measured when the 'optimized' parameters listed in Table 8 were adopted. These values are about the same as those of Ernould et al. (2017), but strain rate effects are not considered in the'Optimized' condition.

Table 8: Parameters used in flat sheet analyses.

| | Optimized | Variations |
|---|---|---|
| Pitch $P$ (mm) | 0.4 | 0.2 |
| Indentation depth $D$ (mm) | 0.2 | 0.1, 0.3 |
| Yield stress $\sigma_o$ [MPa] | 435 | 210, 650 |
| $C_1$ [MPa] | 8.97E+03 | 4.49E+03, 0.0 |
| $C_2$ [MPa] | 1.27E+04 | 6.33E+03, 0.0 |
| $H$ [1/s] | ∞ | 4000 |
| Radius of pin nose $R$ [mm] | 2.0 | 3.0 |

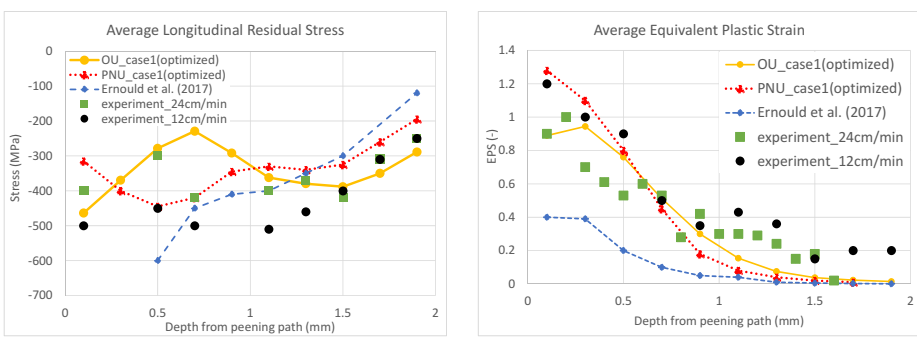


Figure 19: Comparison of residual stress and equivalent plastic strain profiles using optimized parameters with those measured (experiments: measured in Ernould et al. ( 2017)).

Let LRS be RS's longitudinal ($x$-dir.) component. Figure 19 shows comparisons of profiles for RS and equivalent plastic strain (EPS) in through-thickness direction calculated by OU (MSC DYTRAN) and PNU (Abaqus Explicit) using the 'optimized' parameters and those measured. In this figure, averaged LRS and EPS of elements with the same depth on the 5 mm section in model's middle part are plotted. It is shown that RS and EPS calculated in this study agree well with those measured, and FE code dependency is acceptably small. The accuracies of RS near the top face and EPS over the entire area are improved compared with Ernould et al. (2017). These results demonstrates the effectiveness of the adopted FE mesh and 'optimized' parameters in Table 8.

Sensitivity analyses of simulation parameters are performed. Variations in parameters are listed in Table 8. Eleven cases in total listed in Table 9 are examined. The FE mesh of Figure 18 is used. Case 1 is the optimized one which gives the simulation results shown in Figure 19.

Comparisons in RS (and EPS) profiles are shown in Figure 20. The following is found in these analyses:

- Neither RS (for depth < 1mm) and EPS almost never change when the kinematic hardening becomes smaller (Cases 2 and 7).
- RS's peak moves deeper and EPS becomes larger when $D$ becomes larger (Cases 3 and 4) or $R$ becomes larger (Cases 9; Figure 20 (a)).
- RS's absolute value (|LRS|) becomes smaller while EPS almost never change when $\sigma_o$ becomes smaller (Cases 5 and 6; Figure 20 (b)).
- |LRS| raises substantially while EPS almost never change when the strain rate dependency is taken into account (Case 8; Figure 20 (c)).
- Neither RS and EPS almost never change when $P$ becomes smaller (Cases 10 and 11).

Table 9: Parameters given in the sensitivity analyses.

| Case | Pitch $P$ (mm) | | Indentation depth $D$ (mm) | | | Material properties | | | | | | | | Pin radi $R$ (mm) | |
|---|---|---|---|---|---|---|---|---|---|---|---|---|---|---|---|
| | | | | | | Yield Stress $\sigma_o$ (MPa) | | | Hardening coeffs. | | | Strain rate dependency | | | |
| | 0.2 | 0.4 | 0.1 | 0.2 | 0.3 | 210 | 435 | 650 | Optimi-zed | x 0.0 | x 0.5 | Yes | No | 2.0 | 3.0 |
| 1 | | * | | * | | | * | | * | | | | * | * | |
| 2 | | * | | * | | | * | | | * | | | * | * | |
| 3 | | * | | | * | | * | | * | | | | * | * | |
| 4 | | * | * | | | | * | | * | | | | * | * | |
| 5 | | * | | * | | * | | | * | | | | * | * | |
| 6 | | * | | * | | | | * | * | | | | * | * | |
| 7 | | * | | * | | | * | | | | * | | * | * | |
| 8 | | * | | * | | | * | | * | | | * | | * | |
| 9 | | * | | * | | | * | | * | | | | * | | * |
| 10 | * | | | * | | | * | | * | | | | * | * | |
| 11 | * | | | * | | | * | | | * | | | * | * | |

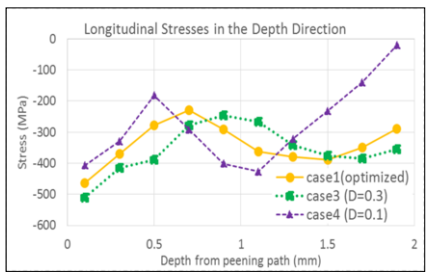


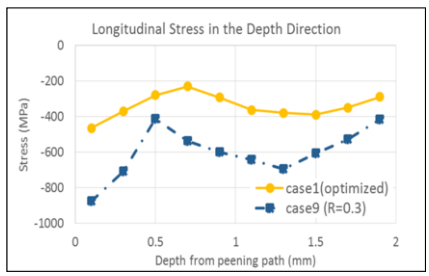


(a) Dependency on indentation depth $D$ and pin's radi $R$.

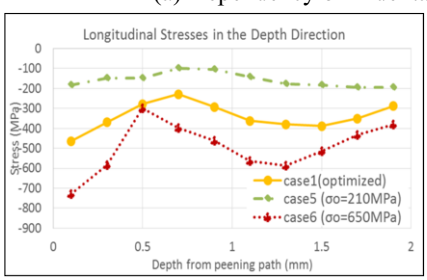


(b) Dependency on yield stress $\sigma_o$.

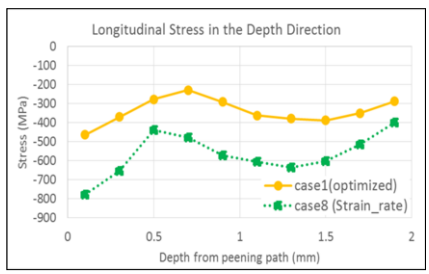


(c) Dependency on strain rate dependency.

Figure 20: Comparisons of residual stress and equivalent plastic strain profiles calculated in the sensitivity analyses.

Hereafter, the FE model of Figure 18 is called 'fine model.' Mesh sensitivity is studied by using 'intermediate model' and 'coarse model,' with larger element size. Let $n_e$ be the number of elements, $l_{min}$ the smallest element's sizes in x, y, z-direction ($n_e$, $l_{min}$) = (105,000, 0.2 x 0.2 x 0.2 mm) for 'fine' model. For compared models, ($n_e$, $l_{min}$) = (20,625, 0.6 x 0.4 x 0.4 mm) for 'intermediate,' and ($n_e$, $l_{min}$) = (4,480, 1.25 x 0.5 x 0.5 mm) for 'coarse' models. The 'Coarse' mesh element size is about the same as that used in the welded joint peening simulation performed by Leitner et al. (2016). This is a typical mesh size adopted in thermal-elasto-plastic welding FE analyses.

For each model, peening responses are calculated using 'optimized' simulation parameters in Table 8. Frequency $f$ = 100Hz Let $l_{min,x}$ be the minimum longitudinal element size. The ratios $l_{min,x}/P$ for fine / intermediate / coarse models are 0.1, 0.3, and 0.625. The comparisons of RS's longitudinal (x-direction) and transversal (y-direction) components, $\sigma_{xx}$ and $\sigma_{yy}$, are shown in Figure 21.

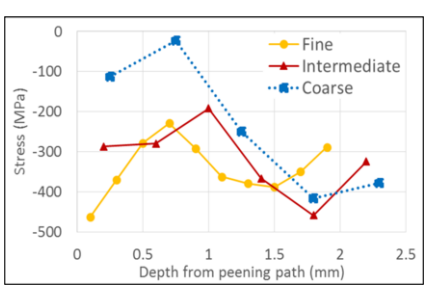


(a) longitudinal component $\sigma_{xx}$

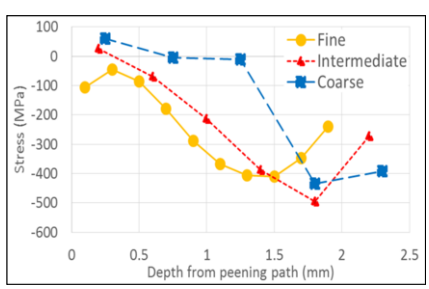


(b) transversal component $\sigma_{yy}$

Figure 21: Comparisons of residual stress components calculated by different meshes.

This figure shows that $\sigma_{xx}$ drastically decreases with the increase in element size (>450MPa for 'fine' mesh, <100MPa for 'coarse' mesh) while the change in $\sigma_{yy}$ is relatively small. This suggests that element size smaller than 1/10 of pin radius should be used if the longitudinal RS becomes a critical.

*6.3.2 Single impact simulation of the HFMI process on stress-free steel sheets*

It takes a lot of man-hour and computational time to perform a 'multiple impact' simulation (MIS) presented above. This man-hour and computational time can be reduced considerably if multiple impacts by a moving pin can be replaced by a single impact by a straight blade. Hereafter, this procedure is called 'single impact' simulation (SIS).

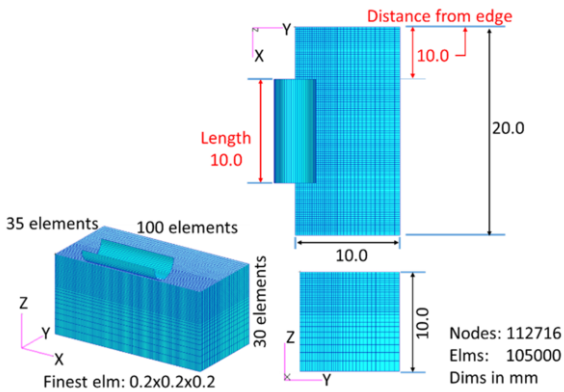


Figure 22: FE mesh of the flat sheet and peening blade used in single impact simulations.

CUT, OU and PNU performed SIS of the steel sheet model. The FE model for SIS is shown in Figure 22. The sheet mesh is the same as that of 'fine' model for MIS. The peening 'blade' with the length of 10 mm is modeled by rigid shell elements. 'Optimized' parameters (excluding pitch $P$) of Table 8 were adopted. For the friction coefficient $\mu$ is 0.30 (same as MIS) and 0.15 (1/2 of MIS). Analyses were performed using different EPFE codes. CUT: Abaqus standard version 6.14.2 (quasi-static), OU: MSC DYTRAN and PNU: Abaqus explicit. Calculated RS profiles are shown in Figure 23. Figure 23 (a) shows calculated averaged longitudinal (LRS) and (b) transversal (TRS) RS. The following are shown in these figures:

- SIS's |LRS| near the top face ranges from -500MPa to -300MPa, which are comparable to the measured ones and the MIS result. However, LRS profiles between 0.5~1.5mm show variations depending on EPFE codes and analysis method (quasi-static vs. explicit). It is also shown that |LRS| near the top face depends on μ.
- SIS's TRS near the top face and TRS profiles show very large variations depending on EPFE codes and analysis method.

These results show that RS calculated by SIS show wide variations depending on EPFE codes and analysis method. More investigations are needed to put SIS HFMI simulation into practical use. Additional experimental data for the transversal RS are also needed.

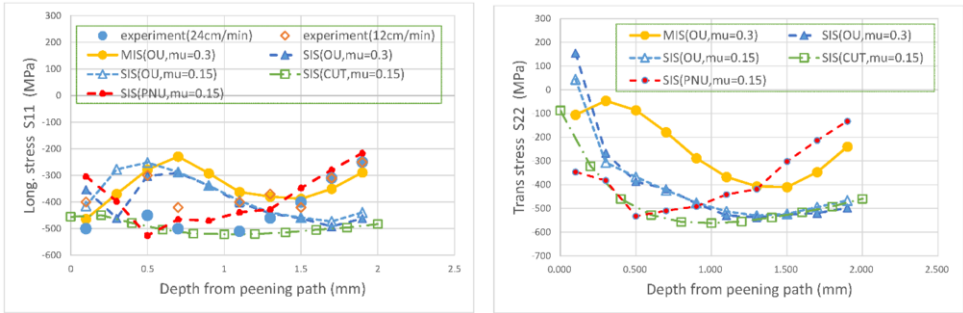


(a) Averaged longitudinal RS. (b) Averaged transversal RS

Figure 23: Comparison of residual stresses calculated by multiple and single impact simulations (experiments: measured in Ernould et al. (2017)).

### *6.3.3 Summary and future plans*

It is shown that the measured RS profile can be reproduced by performing rate-independent explicit displacement controlled FE analysis. The simulation result shows significant mesh sensitivity, and it is found that element size should be smaller than peening pin's radius. Strain hardening does not affect RS profile, but RS's absolute value becomes smaller with the decrease of the yield stress. Both longitudinal and transversal stress profiles can be simulated in multiple impact simulation, while single impact simulation should not be adopted to cases where transversal stress is important. More investigations are needed for the single impact simulation to clarify the transversal stress behaviour. From the benchmark results, a best practice guide with respect to HFMI simulation procedure for the chosen peening tool has been set.

The benchmark group (CUT, OU and PNU) will perform welding-peening simulation of out-of-gusset welded joints following the proposed guideline, and examine the change in RS profile under cyclic loading condition. These results will be published in the near future.

## 7. CONCLUSIONS AND RECOMMENDATIONS

An overview of recent research and development on materials and fabrication technology is presented. Compared to the previous report we have focussed on some new areas, and also refrained from some areas covered in the previous V.3 Committee report, ie line heating, corrosion and simulation based production.

Ship production is still struggling, although with some exceptions like RoRo, cruise and ferries. Also offshore production is very low due to, so far, very low prices on oil. Several legislative initiatives, clean water ballast restrictions, new sulphur emission control area are pushing for a renewal of the fleet. There are also strong research programs on steels and joining methods, and recently on fabricating lighter ships using composites to a larger extent.

The developments of different steels is presented, in particular means of improving the fatigue life for high strength steels. The development of steels and pertinent material properties (eg fracture toughness, CTOD) for use in the arctic is also emphasized, as well as the development of composite materials for marine and subsea applications. We also give some good examples of the use of weight reduction materials.

Welding is still the main joining method for steels. One key outcome of the welding is the distortion of the welded components. With that in mind, several different processes are investigated including use of lower heat input, or use of secondary processes for distortion control. Summarizing, we find that laser beam welding gives the thinnest fusion zone, for the case of butt welding of steel D36. Additive manufacturing is starting to be used also in the maritime sector, we give some examples where it has advantages over other manufacturing methods. Possible applications where additive manufacturing uses automation are also given.

Different manufacturing imperfections appearing in composites have been discussed thoroughly, also joining of composites. Introducing non-crimp fibres are beneficial, it may increase the tensile strength, though it is more expensive than traditional woven rowing. Nano particles which are quite important for the cohesive strength of the matrix (delamination strength and fiber to matrix strength) is also recommended. The infusion method for manufacturing is often better from a cost/benefit analysis when the thickness of the composite is small.

New materials and related fabrication processes offer several benefits like weight saving, integrated functions which may give a reduced life cycle cost of ships and marine structures. However, long term experience of operational performance is not available. The problem of qualification of new materials have been addressed by the V.3 Committee, we arranged a meeting in Hamburg with stakeholders for two European projects, using new materials in ships and classification societies to find what measures that have to be addressed. A suggested best practice for qualification of FRP composites is presented together with a recently issued standard, which opens for several ways of documenting material properties. It also has a multi-scale approach where results from smaller scale tests can be reused for different applications. The use of different levels of verifying material behavior may also limit the number of expensive full-scale long terms tests needed. A survey of qualification and approval processes by different class societies is also given.

The benchmark about the uncertainness in welding simulations indicate good results for the prediction of welding distortions and residual stresses. However, a notable difficulty is the calibration of the equivalent heat course model that required high skilled experts and standards for experimental procedures. A small variation of the model parameters may cause considerable discrepancies on the residual stresses prediction. Moreover, obtaining reliable thermomechanical material properties is a big challenge.

For the adhesive carbon / steel lap joint benchmark, it was found that in general, ADINA tends to overestimate the experimental failure force, while LS-DYNA underestimates it. Good matching is found for axial strains, with better results from ADINA. The failure force is sensitive to $G_c$ (fracture energy) variation, especially in ADINA, while a negligible influence is found for the parameter $k$ (the initial steepness in the cohesive law for the adherend). Use of trilinear or bilinear traction-separation laws lead to comparable results. A similar influence is found for the parameter $\alpha$ (in the mixed mode I and II law) in both software.

For the High Frequency Mechanical Impact (HFMI) benchmark, where peening of a stress-free steel plate (sheet) was simulated numerically, a best practice guide with respect to the HFMI simulation procedure for the chosen peening tool has been set. It was shown that the measured residual stress profiles can be reproduced by performing a rate-independent explicit displacement controlled FE analysis. The simulation results show a significant mesh sensitivity, and it is found that element size should be smaller than peening pin's radius. Strain hardening does not affect the residual stress profiles, but the absolute values of the residual stresses become smaller with the decrease of the yield stress. A complete multiple impact simulation can simulate both longitudinal and transversal stress profiles with good agreement with experiments, while a less computationally intensive single impact simulation should not be adopted to cases where the transversal stress is important.

## REFERENCES

Abaqus/Explicit Reference Manual, 2016, Dassault Systèmes Simulia Corp.

Adam, S. and Ghosh, S., 2016, March. Application of Flexible Composite Pipe as a Cost Effective Alternative to Carbon Steel-Design Experience. In Offshore Technology Conference Asia. Offshore Technology Conference.

Affdl, J.C. and Kardos, J.L., 1976. The Halpin-Tsai equations: a review. Polymer Engineering & Science, 16(5), pp.344-352.

Airoldi, A., Baldi, A., Bettini, P. and Sala, G., 2015. Efficient modelling of forces and local strain evolution during delamination of composite laminates. Composites Part B: Engineering, 72, pp.137-149.

Akpinar, I.A., Gültekin, K., Akpinar, S., Akbulut, H. and Ozel, A., 2017. Research on strength of nanocomposite adhesively bonded composite joints. Composites Part B: Engineering, 126, pp. 143-152.

Akselsen, O.M. and Østby, E., 2014. Evaluation of Welding Consumables for Application down to -60°C. In the 24th International Ocean and Polar Engineering Conference. International Society of Offshore and Polar Engineers.

Akselsen, O.M., Ren, X., Alvaro, A. and Nyhus, B., 2017, July. Key Challenges in Materials and Welding for Application of Steel Structures in Arctic. In The 27th International Ocean and Polar Engineering Conference. International Society of Offshore and Polar Engineers.

An, G.B., Woo, W. and Park, J.U., 2014. Brittle crack-arrest fracture toughness in a high heat-input thick steel weld. International Journal of Fracture, 185(1-2), pp.179-185.

Andena, L., Castellani, L., Castiglioni, A., Mendogni, A., Rink, M. and Sacchetti, F., 2013. Determination of environmental stress cracking resistance of polymers: Effects of loading history and testing configuration. Engineering Fracture Mechanics, 101, pp.33-46.

Anderson, T.A., Fang, B., Attia, M., Jha, V., Dodds, N., Finch, D. and Latto, J., 2016, May. Progress in the Development of Test Methods and Flexible Composite Risers for 3000 m Water Depths. In Offshore Technology Conference. Offshore Technology Conference.

Andideh, M. and Esfandeh, M., 2017. Effect of surface modification of electrochemically oxidized carbon fibers by grafting hydroxyl and amine functionalized hyperbranched polyurethanes on interlaminar shear strength of epoxy composites. Carbon, 123, pp.233-242.

Azzara, A., Rutherford, D. and Wang, H., 2014. Feasibility of imo annex vi tier iii implementation using selective catalytic reduction. International Council on Clean Transportation.

Bai, Z., Song, L., Hu, Y., Gong, X. and Yuen, R.K., 2014. Investigation on flame retardancy, combustion and pyrolysis behavior of flame retarded unsaturated polyester resin with a star-shaped phosphorus-containing compound. Journal of Analytical and Applied Pyrolysis, 105, pp.317-326.

Bajpei, T., Chelladurai, H. and Ansari, M.Z., 2016. Mitigation of residual stresses and distortions in thin aluminium alloy GMAW plates using different heat sink models. Journal of Manufacturing Processes, 22, pp.199-210.

Braura, A. and Mittal, A., 2017. Shipping: Sailing in Troubled Waters, in Global Economic Outlook 2017, 1st Quarter, Deloitte University Press, pp. 56-67.

BRS Group, 2017. Shipping and Shipbuilding Markets – Annual review 2017, www.brsbrokers.com /flipbook en2017.

Caprace, J.D., Fu, G., Carrara, J.F., Remes, H. and Shin, S.B., 2017. A benchmark study of uncertainness in welding simulation. Marine Structures, 56, pp.69-84.

Chaves, V., Beretta, G. and Navarro, A., 2017. Biaxial fatigue limits and crack directions for stainless steel specimens with circular holes. Engineering Fracture Mechanics, 174, pp.139-154.

Chen, L., 2014. Analysis on Situation and Strategy of Chinese Shipbuilding Industry Development. Research Institute of Machinery Industry Economic Management, pp.88-91.

Chen, Y., Tan, L.B., Jaiman, R.K., Sun, X., Tay, T.E. and Tan, V.B.C., 2013, June. Global-local analysis of a full-scale composite riser during vortex-induced vibration. In ASME 2013 32nd International Conference on Ocean, Offshore and Arctic Engineering (pp. V007T08A084-V007T08A084). American Society of Mechanical Engineers.

Chen, Y., Yang, C., Chen, H., Zhang, H. and Chen, S., 2015. Microstructure and mechanical properties of HSLA thick plates welded by novel double-sided gas metal arc welding. The International Journal of Advanced Manufacturing Technology, 78(1-4), pp.457-464.

Colombo, C. and Vergani, L., 2014. Influence of delamination on fatigue properties of a fibreglass composite. Composite Structures, 107, pp.325-333.

Conrardy, C., Huang, T.D., Harwig, D., Dong, P., Kvidahl, L., Evans, N. and Treaster, A., 2006. Practical welding techniques to minimize distortion in lightweight ship structures. Journal of Ship production, 22(4), pp.239-247.

Cricrì, G. and Perrella, M., 2017. Investigation of mode III fracture behaviour in bonded pultruded GFRP composite joints. Composites Part B: Engineering, 112, pp.176-184.

Deng, D., 2009. FEM prediction of welding residual stress and distortion in carbon steel considering phase transformation effects. Materials & Design, 30(2), pp.359-366.

Det Norske Veritas, 2010. Offshore riser system. In: Proceedings of the Offshore service specification. DNV-OSS-302.

Di Landro, L., Montalto, A., Bettini, P., Guerra, S., Montagnoli, F. and Rigamonti, M., 2017. Detection of Voids in Carbon/Epoxy Laminates and Their Influence on Mechanical Properties. Polymers & Polymer Composites, 25(5), p.371.

Ding, D., Shen, C., Pan, Z., Cuiuri, D., Li, H., Larkin, N. and van Duin, S., 2016. Towards an automated robotic arc-welding-based additive manufacturing system from CAD to finished part. Computer-Aided Design, 73, pp.66-75.

Ernould, C., Schubnell, J., Simunek, D., Leitner, M., Maciolek, A., Farajian, M., and Stoschka, M., 2017. Application of Different Simulation Approaches to Numerically Optimize High-Frequency Mechanical Impact (HFMI) Post-Treatment Process, IIW Document XIII-2684-17. International Institute of Welding.

Estefen, S.F., Gurova, T., Castello, X. and Leontiev, A., 2010. Surface residual stress evaluation in double-electrode butt welded steel plates. Materials & Design, 31(3), pp.1622-1627.

European Commission, 2017. CORDIS Community Research and Development Information Service, http://cordis.europa.eu

Evegren, F. and Hertzberg, T., 2017. Fire safety regulations and performance of fibre-reinforced polymer composite ship structures. Proceedings of the Institution of Mechanical Engineers, Part M: Journal of Engineering for the Maritime Environment, 231(1), pp.46-56.

Evegren, F., Rahm, M., Arvidson, M. and Hertzberg, T., 2014. Fire testing of external combustible ship surfaces. Fire Safety Science, 11, pp.905-918.

Foehrenbach J, Hardenacke, V., and Farajian, M., 2016. High Frequency Mechanical Impact Treatment (HFMI) for the fatigue improvement: numerical and experimental investigations to describe the condition in the surface layers, Welding in the World, 60 (4), pp. 749-755.

Gaiotti, M., Rizzo, C.M., Branner, K. and Berring, P., 2014. An high order Mixed Interpolation Tensorial Components (MITC) shell element approach for modeling the buckling behavior of delaminated composites. Composite Structures, 108, pp.657-666.

Gangloff Jr, J.J., Cender, T.A., Eskizeybek, V., Simacek, P. and Advani, S.G., 2017. Entrapment and venting of bubbles during vacuum bag prepreg processing. Journal of Composite Materials, 51(19), pp.2757-2768.

Godani, M., Gaiotti, M. and Rizzo, C.M., 2014. Interlaminar shear strength of marine composite laminates: Tests and numerical simulations. Composite Structures, 112, pp.122-133.

Godani, M., Gaiotti, M. and Rizzo, C.M., 2015, July. Influence of air inclusions on marine composites inter-laminar shear strength. In The Twenty-fifth International Ocean and Polar Engineering Conference. International Society of Offshore and Polar Engineers.

Hahn, H.T. and Tsai, S.W., 1980. Introduction to composite materials. CRC Press.

Han, W.T., Wan, F.R., Li, G., Dong, C.L. and Tong, J.H., 2011. Effect of trailing heat sink on residual stresses and welding distortion in friction stir welding Al sheets. Science and Technology of Welding and Joining, 16(5), pp.453-458.

Harati, E., Karlsson, L., Svensson, L.E. and Dalaei, K., 2017. Applicability of low transformation temperature welding consumables to increase fatigue strength of welded high strength steels. International Journal of Fatigue, 97, pp.39-47.

Harati, E., Svensson, L.E., Karlsson, L. and Widmark, M., 2016. Effect of high frequency mechanical impact treatment on fatigue strength of welded 1300 MPa yield strength steel. International Journal of Fatigue, 92, pp.96-106.

Hase, K., Handa, T. and Eto, T., 2014. Development of YP460 N/mm2 Class Heavy Thick Plate with Excellent Brittle Crack Arrestability for Mega Container Carriers. JFE Technical Report, 20, pp. 8-13.

Hauge, M., Maier, M., Walters, C.L., Østby, E., Kordonets, S.M., Zanfir, C. and Osvoll, H., 2015, July. Status update of ISO TC67/SC8/WG5: Materials for arctic applications. In The Twenty-fifth International Ocean and Polar Engineering Conference. International Society of Offshore and Polar Engineers.

Hazimeh, R., Othman, R., Khalil, K. and Challita, G., 2016. Influence of plies' orientations on the stress distribution in adhesively bonded laminate composite joints subjected to impact loadings. Composite Structures, 152, pp.654-664.

Herzog, D., Seyda, V., Wycisk, E. and Emmelmann, C., 2016. Additive manufacturing of metals. Acta Materialia, 117, pp.371-392.

Holder, R., Larkin, N., Li, H., Kuzmikova, L., Pan, Z. and Norrish, J., 2011. Development of a DC-LSND welding process for GMAW on DH-36 Steel. In 56th WTIA annual conference. Welding Technology Institute of Australia.

Horn, A.M., Østby, E., Moslet, P.O. and Hauge, M., 2016, June. The Fracture Resistance Approach in Order to Prevent Brittle Failure of Offshore Structures Under Arctic Environments. In ASME 2016 35th International Conference on Ocean, Offshore and Arctic Engineering (pp. V004T03A021-V004T03A021). American Society of Mechanical Engineers.

Hüther, J. and Brøndsted, P., 2016, July. Influence of the curing cycles on the fatigue performance of unidirectional glass fiber reinforced epoxy composites. In IOP Conference Series: Materials Science and Engineering (Vol. 139, No. 1, p. 012023). IOP Publishing.

Ilman, M.N., Muslih, M.R., Subeki, N. and Wibowo, H., 2016. Mitigating distortion and residual stress by static thermal tensioning to improve fatigue crack growth performance of MIG AA5083 welds. Materials & Design, 99, pp.273-283.

IMO, 2016. Suitability of High Manganese Austenitic Steel for Cryogenic Service and Development of any Necessary Amendments to the IGC Code and IGF Code, International Maritime Organisation.

Ingalls, 2017. http://www.nmc.ctc.com/index.cfm?fuseaction=projects.details&projectID=288

Jeong, D., Seo, W., Sung, H. and Kim, S., 2016. Near-threshold fatigue crack propagation behavior of austenitic high-Mn steels. Materials Characterization, 121, pp.103-111.

Jesus, J.S., Costa, J.M., Loureiro, A. and Ferreira, J.M., 2017. Fatigue strength improvement of GMAW T-welds in AA 5083 by friction-stir processing. International Journal of Fatigue, 97, pp.124-134.

Jones, R.M., 1998. Mechanics of composite materials. CRC press.

Kalantari, M., Dong, C. and Davies, I.J., 2017. Effect of matrix voids, fibre misalignment and thickness variation on multi-objective robust optimization of carbon/glass fibre-reinforced hybrid composites under flexural loading. Composites Part B: Engineering, 123, pp.136-147.

Kaneko, M. and Tani, T., 2011. Characteristics of Brittle Crack Arrest Steel Plate for Large Heat-input Welding for large Container Ships. Kobelco Technology Review, 30, pp.66-69.

Khurshid, M., Leitner, M., Barsoum, Z., and Schneider, C., 2016. Residual stress state induced by high frequency mechanical impact treatment in different steel grades - Numerical and experimental study. International Journal of Mechanical Sciences, 123, pp. 34-42.

Kim, S.Y., Shim, C.S., Sturtevant, C. and Song, H.C., 2014. Mechanical properties and production quality of hand-layup and vacuum infusion processed hybrid composite materials for GFRP marine structures. International Journal of Naval Architecture and Ocean Engineering, 6(3), pp.723-736.

Knautz, 2017. Procedural principle plasma key hole-welding. URL http://www.schweissmaschinen.net/en/schweissmaschinen/plasma-welding-machines/procedural-principle-plasma-key-hole-welding/ (accessed 2.14.17).

Kobayashi, S., Tsukada, T. and Morimoto, T., 2017. Resin impregnation behavior in carbon fiber reinforced polyamide 6 composite: Effects of yarn thickness, fabric lamination and sizing agent. Composites Part A: Applied Science and Manufacturing, 101, pp.283-289.

Kumar, S. and Nath, S.K., 2016. Effect of heat input on impact toughness in transition temperature region of weld CGHAZ of a HY 85 steel. Journal of Materials Processing Technology, 236, pp.216-224.

Kumar, S. and Shahi, A.S., 2016. Studies on metallurgical and impact toughness behavior of variably sensitized weld metal and heat affected zone of AISI 304L welds. Materials & Design, 89, pp.399-412.

Laitinen, R., Valkonen, I. and Kömi, J., 2013. Influence of the base material strength and edge preparation on the fatigue strength of the structures made by high and ultra-high strength steels. Procedia Engineering, 66, pp.282-291.

Lan, L., Kong, X., Qiu, C. and Zhao, D., 2016. Influence of microstructural aspects on impact toughness of multi-pass submerged arc welded HSLA steel joints. Materials & Design, 90, pp.488-498.

Larkin, N., Pan, Z.X., Van Duin, S., Callaghan, M., Li, H.J. and Norrish, J., 2011. Tandem gas metal arc welding for low distortion butt welds. In Advanced Materials Research (Vol. 337, pp. 511-516). Trans Tech Publications.

Larkin, N., Short, A., Pan, Z. and van Duin, S., 2018. Automated Programming for Robotic Welding. In Transactions on Intelligent Welding Manufacturing (pp. 48-59). Springer, Singapore.

Leitner, M., Khurshid, M., and Barsoum, Z., 2016. Stability of HFMI-treatment induced residual stresses during fatigue. IIW Document XIII-2633-16. International Institute of Welding.

Leitner, M., 2017. Influence of effective stress ratio on the fatigue strength of welded and HFMI-treated high-strength steel joints. International Journal of Fatigue, 102, pp. 158-170.

Levieil, B., Edwards, L., Cortial, F., Sterjovski, Z. and van Duin, S., 2017. Towards thickness reduction and performance improvement: development of low distortion welding processes for naval shipbuilding, FAST 2017, 14th International Conference on Fast Sea Transportation, Nantes, France.

Levieil, B., van Duin, S., Cortial, F., Edwards, L. and Sterjovski, Z., 2017. Low distortion welding for shipbuilding, Pacific 2017, International Maritime Conference, Sydney.

Lin, Y., Jiang, S., Hu, Y., Chen, G., Shi, X. and Peng, X., 2016. Hybrids of aluminum hypophosphite and ammonium polyphosphate: Highly effective flame retardant system for unsaturated polyester resin. Polymer Composites.

Liu, Y., Shi, L., Liu, C., Yu, L., Yan, Z. and Li, H., 2016. Effect of step quenching on microstructures and mechanical properties of HSLA steel. Materials Science and Engineering: A, 675, pp.371-378.

Ma, L. and Liu, D., 2016. Delamination and fiber-bridging damage analysis of angle-ply laminates subjected to transverse loading. Journal of Composite Materials, 50(22), pp.3063-3075.

Maggiani, G., Boote, D., Gaggero, T., Gaiotti, M. and Rizzo, C.M., 2017. Calibration of the Cohesive Parameters of Fiberglass Reinforced Plastic Plates with an Embedded Delamination by Experiments. In The Twenty-seventh International Ocean and Polar Engineering Conference. International Society of Offshore and Polar Engineers.

Marquis, G.B., and Barsoum, Z., 2013. A guideline for fatigue strength improvement of high strength steel welded structures using high-frequency mechanical impact, Procedia Engineering, 66, pp. 98-107.

MARTEC II, 2017. https://www.martec-era.net/index.php?index=21.

Mochizuki, M. and Toyoda, M., 2007. Weld distortion control during welding process with reverse-side heating. Journal of Engineering Materials and Technology, 129(2), pp.265-270.

Mochizuki, M., Yamasaki, H., Okano, S. and Toyoda, M., 2006. Distortion behaviour of fillet T-joint during in-process control welding by additional cooling. Welding in the World, 50(5-6), pp.46-50.

MSC Software. 2017. MSC DYTRAN2017 Reference Manual.

Muren, J., Caveny, K., Eriksen, M., Müller-Allers, J., Engelbreth, K.I. and Eide, J., 2013. Petroleum Safety Authority Norway: Un-bonded Flexible Risers–Recent Field Experience and Actions for Increased Robustness.

Nagy, T., 2012. Investigation of thermal techniques to mitigate buckling distortion in welding panels. Cranfield University, UK.

O'Brien, R., Veldsman, W. and Elmarakbi, A., 2015. The development of an industrial robotic Low Stress No Distortion (LSND) welding system. The IIW International Conference on High Strength Materials - Challenges and Applications, Helsinki. International Institute of Welding.

Okano, S. and Mochizuki, M., 2016. Experimental and Numerical Investigation of Trailing Heat Sink Effect on Weld Residual Stress and Distortion of Austenitic Stainless Steel. ISIJ International, 56(4), pp.647-653.

Olave, M., Vara, I., Husabiaga, H., Aretxabaleta, L., Lomov, S.V. and Vandepitte, D., 2015. Nesting effect on the mode I fracture toughness of woven laminates. Composites Part A: Applied Science and Manufacturing, 74, pp.166-173.

Ottersböck, M.J., Leitner, M., Stoschka, M. and Maurer, W., 2016. Effect of Weld Defects on the Fatigue Strength of Ultra High-strength Steels. Procedia Engineering, 160, pp.214-222.

Pallaspuro, S., Yu, H., Kisko, A., Porter, D. and Zhang, Z., 2017. Fracture toughness of hydrogen charged as-quenched ultra-high-strength steels at low temperatures. Materials Science and Engineering: A, 688, pp.190-201.

Park, J.Y. and Kim, M.H., 2016, June. Fatigue Crack Propagation Characteristics of 3.5 to 9 wt% Nickel Steels for Low Temperature Applications. In ASME 2016 35th International Conference on Ocean, Offshore and Arctic Engineering (pp. V004T03A010-V004T03A010). American Society of Mechanical Engineers.

Park, S.J., Heo, G.Y. and Jin, F.L., 2015. Cure behaviors and thermal stabilities of tetrafunctional epoxy resin toughened by polyamide. Macromolecular Research, 23(4), pp.320-324.

Pazooki, A.M.A., Hermans, M.J.M. and Richardson, I.M., 2017. Control of welding distortion during gas metal arc welding of AH36 plates by stress engineering. The International Journal of Advanced Manufacturing Technology, 88(5-8), pp.1439-1457.

Pérez-Mora, R., Palin-Luc, T., Bathias, C. and Paris, P.C., 2015. Very high cycle fatigue of a high strength steel under sea water corrosion: A strong corrosion and mechanical damage coupling. International Journal of Fatigue, 74, pp.156-165.

Pham, D.C., Sridhar, N., Qian, X., Sobey, A.J., Achintha, M. and Shenoi, A., 2016. A review on design, manufacture and mechanics of composite risers. Ocean Engineering, 112, pp.82-96.

Saat, A.M., Malik, A.A., Azmi, A., Latif, M.F.A., Ramlee, N.E. and Johan, M.R., 2017. Effect of aluminum phosphate on mechanical and flame retardant properties of composites fiberglass. ARPN Journal of Engineering and Applied Sciences, 12, pp. 1315-1318.

Scheid, A., Félix, L.M., Martinazzi, D., Renck, T. and Kwietniewski, C.E.F., 2016. The microstructure effect on the fracture toughness of ferritic Ni-alloyed steels. Materials Science and Engineering: A, 661, pp.96-104.

SEA Europe, 2017. Shipbuilding market monitoring report No 42, SEA Europe – Shipyards & Maritime Equipment Association (www.seaeurope.nu).

Shen, C., 2013. Low distortion welding for shipbuilding industry. University of Wollongong, Australia

Shengsun, H., Guo, C., Wang, D., and Wang, Z., 2016. 3D Dynamic Finite Element Analysis of the Nonuniform Residual Stress in Ultrasonic Impact Treatment Process, Journal of Materials Engineering of Performance, 25, pp. 4004-4015.

Shenoi, R.A. and Wellicome, J.F. eds., 1993. Composite Materials in Maritime Structures: Volume 1, Fundamental Aspects. Cambridge University Press.

Shibanuma, K., Yanagimoto, F., Namegawa, T., Suzuki, K. and Aihara, S., 2016. Brittle crack propagation/arrest behavior in steel plate–Part I: Model formulation. Engineering Fracture Mechanics, 162, pp.324-340.

Shiino, M.Y., Pelosi, T.S., Cioffi, M.O.H. and Donadon, M.V., 2017. The Role of Stitch Yarn on the Delamination Resistance in Non-crimp Fabric: Chemical and Physical Interpretation. Journal of Materials Engineering and Performance, 26(3), pp.978-986.

Shiozaki, T., Tamai, Y. and Urabe, T., 2015. Effect of residual stresses on fatigue strength of high strength steel sheets with punched holes. International Journal of Fatigue, 80, pp.324-331.

Skriko, T., Ghafouri, M. and Björk, T., 2017. Fatigue strength of TIG-dressed ultra-high-strength steel fillet weld joints at high stress ratio. International Journal of Fatigue, 94, pp.110-120.

Soderhjelm, C. and Apelian, D., 2016. Metallurgical bonding between cast-in ferrous inserts and aluminum, La Metallurgia Italiana, 6, pp. 93-100.

Song, K., Dávila, C.G. and Rose, C.A., 2008, May. Guidelines and parameter selection for the simulation of progressive delamination. In ABAQUS User's Conference (Vol. 41, pp. 43-44).

Song, S.W., Kwon, Y.J., Lee, T. and Lee, C.S., 2016a. Effect of Al addition on low-cycle fatigue properties of hydrogen-charged high-Mn TWIP steels. Materials Science and Engineering: A, 677, pp.421-430.

Song, S.W., Lee, J.H., Lee, H.J., Bae, C.M. and Lee, C.S., 2016b. Enhancing high-cycle fatigue properties of cold-drawn Fe–Mn–C TWIP steels. International Journal of Fatigue, 85, pp.57-64.

Sproesser, G., Pittner, A. and Rethmeier, M., 2016. Increasing performance and energy efficiency of gas metal arc welding by a high power tandem process. Procedia CIRP, 40, pp.642-647.

Sterjovski, Z., Donato, J., Munro, C., Luzin, V., Lane, N., and Larkin, N., 2011. An evaluation of pulsed tandem gas metal arc welding of high-strength HSLA65 steel for naval shipbuilding, In 56th WTIA annual conference. Welding Technology Institute of Australia.

Sudheesh, R.S. and Prasad, N.S., 2015. Comparative Study of Heat Transfer Parameter Estimation Using Inverse Heat Transfer Models of a Trailing Liquid Nitrogen Jet in Welding. Heat Transfer Engineering, 36(2), pp.178-185.

Sutherland, L.S., Amado, C. and Soares, C.G., 2017. Statistical experimental design techniques to investigate the strength of adhesively bonded T-joints. Composite Structures, 159, pp.445-454.

Tan, L.B., Chen, Y., Jaiman, R.K., Sun, X., Tan, V.B.C. and Tay, T.E., 2015. Coupled fluid–structure simulations for evaluating a performance of full-scale deepwater composite riser. Ocean Engineering, 94, pp.19-35.

Thompson, A.M., Dilthey, U., Fersini, M., Richardson, I., Dos Santos, J., Yapp, D. and Hedegård, J., 2008. Improving the competitiveness of the European steel fabrication industry using synchronised tandem wire welding technology. Brussels: European Commission, Directorate-General for Research, Research Fund for Coal and Steel Unit.

Tomaso, E., Risso, G., Gaiotti, M. and Rizzo, C.M., 2014, August. Numerical Simulation Strategies of Single Lap Joints. In The Twenty-fourth International Ocean and Polar Engineering Conference. International Society of Offshore and Polar Engineers.

Udvardy, S., Nuechterlein, J. and Makhlouf M., 2012, Development of High Performance Nano-Composite Materials, North America Die Casting Association, Super Weapons Systems through castings Report, pp. 133-148.

Usami, A., Kishimoto N., Kusumoto H., Kaneko F. and Inoue T., 2016. Cryogenic leakage risk analysis for FLNG and use of brittle crack arresting material as a risk mitigation measure, Proceedings of the Society for Naval Architects and Marine Engineers.

Van der Aa, E.M., 2007. Local cooling during welding: prediction and control of residual stresses and buckling distortion. Delft University of Technology, The Netherlands..

Wang, X.L., Nan, Y.R., Xie, Z.J., Tsai, Y.T., Yang, J.R. and Shang, C.J., 2017. Influence of welding pass on microstructure and toughness in the reheated zone of multi-pass weld metal of 550 MPa offshore engineering steel. Materials Science and Engineering: A, 702, pp.196-205.

Wang, X.Y. and Whitworth, J.R., 2016. Using additive manufacturing to mitigate the risks of limited key ship components of the Zumwalt-class destroyer (Doctoral dissertation, Monterey, California: Naval Postgraduate School).

Vargas, M.A., Vázquez, H. and Guthausen, G., 2015. Non-isothermal curing kinetics and physical properties of MMT-reinforced unsaturated polyester (UP) resins. Thermochimica Acta, 611, pp.10-19.

Wei, H.L., Li, H., Gao, Y., Ding, X.P. and Yang, L.J., 2015. Welding process of consumable double electrode with a single arc GMAW. The International Journal of Advanced Manufacturing Technology, 76(1-4), pp.435-446.

Wilkins, J., 2016, May. Qualification of Composite Pipe. In Offshore Technology Conference.

Woo K., Nelson J.W., Cairns D.S. and Riddle T.W., 2013. Effects of Defects: Part B—Progressive Damage Modeling of Fiberglass/Epoxy Composite Structures with Manufacturing Induced Flaws Utilizing Cohesive Zone Elements. In 54th AIAA/ASME/ASCE/AHS/ASC Structures, Structural Dynamics, and Materials Conference 2013 Apr (p. 1628).

World Industrial Reporter, 2017. https://worldindustrialreporter.com/port-of-rotterdam-uses-3d-printing-to-repair-damaged-ship-parts/.

Yaacob, M., Zakaria, I., Koto, J., Zarina, P. and Mun'aim, M.A.M.K., 2017. Comparative mechanical properties study of resin infusion versus hand laminating for the construction of 12-ft fishing boat. ARPN Journal of Engineering and Applied Sciences, 12, pp. 1954-1960.

Yang, C., Zhang, H., Zhong, J., Chen, Y. and Chen, S., 2014. The effect of DSAW on preheating temperature in welding thick plate of high-strength low-alloy steel. The International Journal of Advanced Manufacturing Technology, 71(1-4), pp.421-428.

Yasuda, A., and Rashed, S., 2016. Efficient Collapse Analysis of Ductile Components Subjected to Impact Loads in ASME 2016 35nd International Conference on Ocean, Offshore and Arctic Engineering, paper OMAE2016-54480. American Society of Mechanical Engineers.

Yildirim, H.C. and Marquis, G.B., 2012. Fatigue strength improvement factors for high strength steel welded joints treated by high frequency mechanical impact. International Journal of Fatigue, 44, pp.168-176.

Zhang, H., Zhang, G., Cai, C., Gao, H. and Wu, L., 2008. Fundamental studies on in-process controlling angular distortion in asymmetrical double-sided double arc welding. Journal of Materials Processing Technology, 205(1), pp.214-223.

Østby, E., Akselsen, O.M., Hauge, M. and Horn, A.M., 2013, June. Fracture mechanics design criteria for low temperature applications of steel weldments. In The Twenty-third International Offshore and Polar Engineering Conference. International Society of Offshore and Polar Engineers.

Østby, E., Hauge, M. and Horn, A.M., 2015, July. Development of materials requirement philosophies for design to avoid brittle behaviour in steel structures under Arctic conditions. In The Twenty-fifth International Ocean and Polar Engineering Conference. International Society of Offshore and Polar Engineers.